A *Catharanthus roseus* mutant with trace levels of secologanin and monoterpenoid indole alkaloids does not express BIS1/BIS2 transcription factors and fails to activate iridoid biosynthesis.

By

Trevor Kidd, Hons. B.Sc.

Submitted to the Department of Biotechnology

In partial fulfillment of the requirements

For the degree of

Masters of Science

Brock University

St. Catharines, Ontario

2016

Abstract

The Madagascar periwinkle (*Catharanthus roseus)* is the sole source of the monoterpenoid indole alkaloids (MIAs) that result in several essential anti-cancer chemotherapies as well as being an important source for other MIA derived pharmaceutical agents. Most of the alkaloid and pre-alkaloid iridoid pathway has been elucidated, but some critical areas remain uncharacterized. The early iridoid pathway is localized to internal phloem associated parenchyma (IPAP) cells, with the latter part of the pathway localized to the epidermal cells indicating intercellular transport within the leaf tissue does occur. However, possible transport or translocation of MIAs or pre-MIAs between organs within *Catharanthus roseus* has not been studied.

Previously, 3600 EMS (ethyl methane sulfonate) mutagenized *C. roseus* plants had been screened with a simple TLC (thin layer chromatography) to identify mutants with altered MIA profiles yielded one plant with trace MIA production. This trace MIA status was confirmed using UPLC-MS (Ultra Performance Liquid Chromatography and Mass Spectrometry) and the plant had a thick, stocky, short root system, small leaves, a rigid stem, premature senescence and was susceptible to infection resulting in its rescue to in-vitro.

Quantitative real-time PCR analysis of iridoid gene expression showed significant downregulation of several iridoid pathway genes as well as the downregulation of transcription factors BIS1 and BIS2.

Feeding the trace MIA mutant roots the iridoid secologanin resulted in alkaloid production in the leaves. While grafting trace MIA mutant shoots onto MIA producing WT roots also resulted in alkaloid production in the mutant leaves.

This study establishes that MIAs or pre-MIA iridoids, such as secologanin, may be translocated between the plant organs and this may be useful for the identification of novel transporters, enzymes, and transcription factors.

Acknowledgements

I would like to start by thanking my supervisor Dr Vincenzo De Luca for giving me the opportunity to work in his lab. The support and guidance he gave me were invaluable. Next, I would like to thank my committee members Dr Jeffrey Atkinson and Dr David Liscombe for their support and advice along the way.

I am grateful to the members of my lab, especially Dr Paulo Cazares who took me under his wing when I arrived, Dr Yang Qu for his for his endless guidance and ideas, and Dr Kyung-Hee Kim for help with the UPLC-MS. Also Dr Brent Weins, Alison Edge, Michael Easson, Dr Zerihum Demissie, Kimberley Catherine, Graham Jones, Danielle Williams, Bader Abu-Omar and Olga Safonova for making my time in the lab more memorable.

Finally, I would like to thank my Fiancé Patricia McNeil for her love and support. My parents for always being there when I needed some help, and my family and friends. Thank you all.

Contents

List of Figures

List of Tables

List of Abbreviations

7DLS	7-deoxyloganic acid synthase
8-HGO	8-hydroxygeraniol oxidoreductase
10-HGO	10-hydroxygeraniol oxidoreductase
16OMT	16-hydroxytabersonine-16-O-methyltransferase
ABC	ATP-binding cassette
bHLH	basic Helix-Loop-Helix
BIS	bHLH transcription factor
CA	cathenamine reductase
cDNA	complementary DNA
cMEPP	2-C-methyl-D-erythritol-2,4-cyclodiphosphate
CR	Cathenamine reductase
CrP5βR	progesterone 5β reductase-like
CYP	cytochrome P450
D4H	deacetoxyvindoline 4-hydroxylase
DAT	deacetylvindoline O-acetyltransferase
DEPC	diethylpyrocarbonate
DL7H	7-deoxyloganic acid 7-hydroxylase
DLGT	deoxyloganic acid glucosyltransferase
DMAPP	dimethylallyl diphosphate
DNA	deoyribonucleic acid
DXP	1-deoxy-D-xylylose-5-phosphate
DXR	1-deoxy-D-xylulose-5-phosphate reductase
DXS	1-deoxy-D-xylulose-5-phosphate synthase
EDTA	ethylenediaminetetraacetic acid
EMS	ethyl methane sulphonate
ENU	1-ethyl-1-nitrosourea
FAO/IAEA	Food and Agriculture Organisation/International Atomic Energy Agency
G10H	geraniol 10-hydroxylase
GES	geraniol synthase
GPP	geraniol diphosphate
GS	geraniol synthase
HDR	HMBPP reductase
HDS	hydroxymethyl butenyl diphosphate synthase
HMBPP	1-hydroxy-2-methyl-2-(E)-butenyl 4-phosphate
HMG-CoA	3-hydroxy-3-methylglutaryl-coenzyme A
HMGR	3-hydroxy-3-methylglutaryl-coenzyme A reductase
HPLC	high-performance liquid chromatography
IAA	indole-3-acetic acid
IPAP	internal phloem-associated parenchyma
IPP	isopentenyl diphosphate
IS	iridoid synthase
LAMT	loganic acid O-methyltransferase
MATE	multidrug and toxic compound extrusion

MCS	2-C-methyl-D-erythritol 2,4-cyclodiphosphate synthase
MeJA	methyl jasmonate
MEP	methylerythritol 4-phosphate
MIA	monoterpenoid indole alkaloid
MNU	1-methyl-1-nitrosourea
MS	mass spectrometry
MS	Murashige and Skoog
MVA	mevalonic acid
NAA	1-Napthaleneacetic acid
NADPH	nicotinamide adenine dinucleotide phosphate
NMT	16-methoxy-2,3-dihydro-3-hydroxytabersonine N-methyltransferase
Nt-JAT	jasmonate-inducible alkaloid transporter
NUP	nicotine uptake permease
ORCA	octadecanoid-responsive Catharanthus APETALA2-domain
P5βR	progesterone 5β reductase-like
PCR	polymerase chain reaction
PUP	purine permease
qPCR	real-time polymerase chain reaction
qRT-PCR	quantitative reverse transcriptase-polymerase chain reaction
RNA	ribonucleic acid
SGD	strictosidine β-D-glucosidase
SLS	secologanin synthase
SNP	single nucleotide polymorphism
STR	strictosidine synthase
T3O	tabersonine 3-oxidase
T3R	tabersonine 3-reductase
T16H	tabersonine 16-hydroxylase
TDC	tryptophan decarboxylase
TILLING	targeting induced local lesions in the genomes
TLC	thin layer chromatography
UGT8	UDP deoxyloganetic acid-glycosyltransferase
UPLC-MS	ultra-performance liquid chromatography-mass spectrometry
VIGS	virus-induced gene silencing
WT	Wild Type - *Catharanthus roseus* variety Pacifica Peach, parental line

1 Literature Review

1.1 *Catharanthus roseus* and monoterpenoid indole alkaloids

Catharanthus roseus (L.) G. Don is an extensively studied medicinal plant commonly known as Madagascar periwinkle belonging to the Apocynaceae family (Van Der Heijden, Jacobs, Snoeijer, Hallard, & Verpoorte, 2004). Research with this plant has focused on the biological activity, chemistry, biochemistry and molecular biology of several unique pharmacologically important monoterpenoid indole alkaloids (MIAs) that it produces. The above-ground parts of the plant accumulate small amounts of the dimeric MIA α-3,4-anhydrovinblastine that is chemically converted to the anticancer drugs vinblastine and vincristine. These plant derived MIAs remain the only commercial source for production of these two potent anticancer chemotherapies, while the roots system accumulates ajmalicine and serpentine that have found use in treating hypertension (Van Der Heijden et al., 2004). These four MIAs are among almost 130 MIAs found in *Catharanthus roseus.*

The term, alkaloid, initially defined as "a pharmacologically active, nitrogen-containing basic compounds of plant origin" has been expanded since they also occur in animals (Buchanan, Gruissem, & Jones, 2015). In addition, many alkaloids are not pharmacologically active, and others are not basic. A more generic definition would be "Alkaloids are low-molecular-weight natural products, mainly aromatic secondary metabolites, which contain nitrogen" (Buchanan et al., 2015). More than twenty thousand alkaloids (Buchanan et al., 2015) have been identified across all species, and they are found in roughly 20% of all plant species but more predominantly within the Solanaceae, Papaveraceae, Apocynaceae and Ranunculaceae families (Shitan, Kato, &

Shoji, 2014). Since alkaloid chemistry is highly varied and biologically active, plants often store them in vacuoles within the cell to avoid their toxicity (Mithöfer & Boland, 2012). Herbivory releases the toxins from vacuoles and ingestion by herbivores affects their metabolism by inhibiting enzymes that control neurological function, cell division, ion transport and a myriad of other physiological processes (Mithöfer & Boland, 2012).

While alkaloids are found in one-fifth of all plant species, the over 3000 MIAs that have been identified occur mainly in thousands of species within the Apocynaceae, Loganiaceae and Rubiaceae families (Facchini & De Luca, 2008; Van Der Heijden et al., 2004). MIAs differ from other alkaloids since they are derived from the condensation of tryptamine and a class of terpenoids known as iridoids. They are often found in plants as glycosides, and more than 800 structures are known. While the function of iridoids is not currently well known, early studies have linked them to defense against insect herbivory (Beninger, Cloutier, Monteiro, & Grodzinski, 2007) as shown by catalpol, catalposide, aucubin, loganin and asperuloside that all hinder the growth of gypsy moth larvae (Beninger, Cloutier, & Grodzinski, 2008). Phytochemical studies with *Plantago lanceolata* showed that iridoid levels were highest in the youngest tender and nutrient rich leaves that were likely the most valuable photosynthetically active parts of the plant (Beninger et al., 2007).

1.1.1 The use of EMS for selection of useful traits and targeted improvement plants used by humans

During the past century breeding programs for crop improvement have increasingly used mutation breeding to create new varieties with desirable traits such as increased yields and

quality of the crop. A key strategy did not require high genetic diversity and involved mutagenesis of well understood existing commercial varieties followed by the selection of the desired traits and their introgression through breeding to develop superior crops (Sikora, Chawade, Larsson, Olsson, & Olsson, 2011). The first technique involved the use of X-ray radiation in 1927 that increased the mutation rate by 15,000% in *Drosophila melanogaster*, while it triggered sterility and enhanced phenotypic variation in barley (Sikora et al., 2011). The use of chemical mutagens was pioneered in the 1940s in search for methods that produced the most genetic variation while minimizing increased viability of the biological material (Shu, Forster, & Nakagawa, 2012; Sikora et al., 2011). Compared to radiation techniques, chemical mutagens are technically easier to use and provide high mutation rates while causing far less genomic damage that would reduce viability. Chemical mutagens tend to generate single-nucleotide polymorphisms (SNPs) instead of deletions and translocations associated with radiation treatments (Sikora et al., 2011).

Many compounds have been found to induce mutations in eukaryotic and prokaryotic cells. In plants alkylating agents, including ethyl methane sulphonate (EMS), 1-methyl-1-nitrosourea (MNU) and 1-ethyl-1-nitrosourea (ENU), have been used in plant breeding research (Shu, Forster, & Nakagawa, 2012). Research studies with *Nicotiana tabacum* leaves have shown that between MNU, ENU, and EMS, EMS has the lowest mutagenic potency and the lowest DNA damaging activity (Shu, Forster, & Nakagawa, 2012). As a result, EMS has seen the greatest use in developing large mutagenized plant populations for screening induced phenotypically expressed mutations and has been facilitated recently in a procedure referred to as TILLING (targeting induced local lesions in the genomes) (Shu, Forster, & Nakagawa, 2012). EMS results in random point mutations where the alkylation of guanine residues in DNA results

in the formation of O6-alkylguanine that pairs with thymine instead of cytosine. With subsequent DNA repair, the O6-alkylguanine is replaced with an adenine and overall the original G/C pair has been replaced with an A/T pair. However, a small percentage - 1 to 2% - of point mutation involves a "transversion" converting an A/T to a G/C pair. Missense mutations are the most common result of these point mutations (65%) with another 30% being silent mutations and 5% introducing stop codons (McCallum, Comai, Greene, & Henikoff, 2000).

In the past 80 years, thousands of plant mutants have been released to be used for breeding programs or have led to the development of novel commercial varieties of field or fruit crop (Ahloowalia, Maluszynski, & Nichterlein, 2004). Mutagenesis has also greatly diversified the array of mutations with novel genetic characteristics that are being used in plant breeding programs around the world. The joint FAO/IAEA division lists 3234 crop cultivars in which at least one useful trait is derived from induced mutation, including wheat, barley, rice, cotton, and grapefruit varieties. At least forty cultivars were developed in Canada that includes varieties of sweet cherry, barley, flax, apple, oat and rapeseed (FAO-IAEA, 2016).

1.1.2 EMS mutagenesis has been used to target the MIA chemistry of *Catharanthus roseus*

EMS has been used with limited success by several research groups to generate mutagenized populations of *C. roseus* with the goal of increasing MIA production. The value of EMS or g-ray treatment to induce mutations in *C. roseus* has recently been compared (Mangaiyarkarasi et al., 2014). EMS exceeded g-ray treatments to induce chlorophyll mutations that generated albino (white) and xantha (yellow) mutant leaves with an increase in mutation frequency associated with dose.

Several studies have been conducted on the cytological effects of EMS on *Catharanthus roseus* root tip cells. Verma et al. (2012) used treatment of roots with EMS which produced a dose-dependent increase in the mitotic index, where a 0.5% dose increased the percentage of dividing cells with abnormalities by ca 13-fold. Smaller, but consistent increases were observed as the dose increased to 0.75% (15-fold) and 1% (16-fold) (Verma, Singh, & Singh, 2012). In a separate study lower concentrations of EMS treatment were shown to be as effective (Rani & Kumar, 2015), while both studies found the EMS treatment of roots increased the incidence of chromosomal anomalies (clumping stickiness, tropokinesis, condensation, persistent nucleolous, fragmentation, C-metaphase, triploid cell, bridge, laggard, cleft and binucleoated cells) (Mangaiyarkarasi et al., 2014; Rani & Kumar, 2015).

While mutation breeding efforts to increase MIA content in *C. roseus* roots and leaves have been ongoing for several decades, success has been limited. One successful effort led to the identification of 3 EMS mutants with high root MIA content and 1 EMS mutant with 30% higher leaf MIA content following EMS mutagenesis of the *C. roseus* variety named Nirmal (Kulkarni & Baskaran, 2015; Kulkarni, Baskaran, Chandrashekara, & Kumar, 1999) that is only available in India. The same research group identified two more mutants with increased leaf and root MIAs. Crosses of the two mutants ("necrotic leaf" and "nerium leaf") generated a double-mutant with 33% higher MIA levels than either parent. When differences in the leaf size were taken into account the increased MIA content was nullified (Kulkarni & Baskaran, 2015).

Despite these setbacks, the present thesis shows that simple TLC based screening techniques can be useful to identify altered MIA *Catharanthus roseus* mutants in greenhouse cultivated plants within relatively short periods.

1.2 The Biosynthesis of monoterpenoid indole alkaloids

The largest class of secondary metabolites are the terpenes of which there are approximately 25,000 compounds (Zwenger & Basu, 2008) found in higher plants alone. They display a wide range of biological functions including involvement in photosynthesis, electron transport, precursors to several hormones and attractants as well as deterrents (Bowsher, Steer, & Tobin, 2008; Rodríguez-Concepción & Boronat, 2002). One or more isoprene units, joined in various orientations, constitute all terpenes, with single units (5 carbon) being called hemiterpenes; two units (C10) forming monoterpenes; three unit (C15) sesquiterpenes; four unit (C20) diterpenes, six unit (C30) triterpenes, and 8 units (C40) tetraterpenes (Bowsher et al., 2008). The two unit monoterpenes were the first discovered and given the singular name despite being formed from two five-carbon units (Bowsher et al., 2008).

The biosynthesis of MIAs in *C. roseus* is long and complex involving many reactions that have been divided into 4 different stages**: *i,*** The production of isopentenyl pyrophosphate (IPP) through the mevalonate (MVA) and/or methylerythritol pyrophosphate (MEP) pathways; ***ii,*** The early pathway - iridoid pathway; ***iii;*** The mid-pathway and ***iv,*** The late pathway.

1.2.1 The production of IPP through the MVA and/or MEP pathway

There are two different pathways that result in IPP formation in higher plants, the mevalonic acid (MVA) pathway, and the methylerythritol 4-phosphate (MEP) pathway. The MVA pathway, localized in the cytosol, was discovered in the 1960s and was long considered to be the only pathway for the formation of IPP until the discovery of the MEP pathway in bacteria roughly 30 years later. Higher plants possess cytosol-localized MVA and plastid-localized MEP pathways, while animals, fungi, archaebacteria, and some eubacteria only possess the MVA

pathway and most eubacteria and green algae only possess the MEP pathway (Bowsher et al., 2008; Rodríguez-Concepción & Boronat, 2002). In plants, the cytosol located MVA pathway supplies the IPP for biosynthesis of sesquiterpenes and triterpenes, while the plastid-localized MEP pathway supplies IPP for monoterpene, diterpene and tetraterpene biosynthesis (El-Sayed & Verpoorte, 2007; Lange & Croteau, 1999). While both pathways appear to be involved in crosstalk and participation in supplying precursors for various biological processes, isotope feeding studies with *C. roseus* suggest that the plastid-localized MEP pathway supplies most of the IPP for MIA biosynthesis (Contin, Van Der Heijden, Lefeber, & Verpoorte, 1998; El-Sayed & Verpoorte, 2007; Lichtenthaler, 1999).

The biochemical reactions of the mevalonate pathway

The mevalonate acid pathway produces the end product IPP from acetyl-CoA. It begins with condensation of two acetyl-CoA molecules to form acetoacetyl-CoA, catalyzed by acetoacetyl-CoA thiolase. To that product, another molecule of acetyl-CoA is added to form 3-hydroxy-3-methylglutraryl-CoA (HMG-CoA) catalyzed by HMG-CoA synthase. The HMG-CoA is subsequently reduced by HMG-CoA reductase HMGR to form MVA. The next two steps are both phosphorylation, with mevalonate kinase and 5-phosphomevalonate kinase producing mevalonate diphosphate which is subsequently decarboxylated by 5-diphosphomevalonate decarboxylase to IPP (Bowsher et al., 2008; Lange & Croteau, 1999).

The biochemical reactions for Methyl Erythritol Phosphate (MEP) Pathway

The MEP pathway converts glyceraldehyde-3-phosphate and pyruvate to IPP, as well as the IPP isomer DMAPP, through a series of steps.

The pathway begins with the condensation of glyceraldehyde-3-phosphate with pyruvate to form 1-deoxy-D-xylylose-5-phosphate (DXP) catalyzed by deoxy-xylulose-5-phophate synthase (DXS). In that forming of DXP two carbon units are transferred from pyruvate to the glyceraldehyde-3-phosphate in a transketolase decarboxylation reaction (Bowsher et al., 2008; Chahed et al., 2000; Phillips, Leon, Boronat, & Rodriguez-Concepcion, 2008).

The next part of the pathway involves two steps. The first in which DXP is converted to 2-C-methyl-erythrose-4-phosphate and then the second involves that intermediate being reduced to 2-C-methyl-D-erythritol-4-phosphate (MEP). Both steps are mediated by the reductoisomerase enzyme DXR (Bowsher et al., 2008; Phillips et al., 2008). CTP condenses the MEP to 4-(cytidine 5´-diphospho)-2-C-methyl-D-erythritol (Phillips et al., 2008) which in turn is phosphorylated by an ATP-dependent kinase reaction forming 2-phospho-4-(cytidine 5´diphospho)-2-C-methyl-D-erythritol (El-Sayed & Verpoorte, 2007).

The cytidine monophosphate is removed in the next step by 2-C-methyl-D-erythritol-2,4-cyclodiphosphate synthase (MCS) while the two remaining phosphate groups from a cyclic structure 2-C-methyl-D-erythritol-2,4-cyclodiphosphate (cMEPP). The ring is then reopened in the following reaction catalyzed by hydroxymethyl butenyl diphosphate synthase (HDS) where cMEPP is reduced forming the linear structure 1-hydroxy-2-methyl-2-(E)-butenyl 4-phosphate (HMBPP). The final step is catalyzed by HMBPP reductase (HDR) to form IPP and its isomer DMAPP (Bowsher et al., 2008). However, in preparation for the iridoid pathway, two more steps are required. First, the monoterpene precursor geranyl diphosphate (GPP) is formed from the condensation of DMAPP with one IPP. GPP is then catalyzed by geraniol synthase (GS) forming geraniol (Contin et al., 1998).

1.2.2 The early pathway: Iridoid biosynthesis

The MEP and iridoid pathways leading to the formation of loganic acid are preferentially expressed in specialized internal phloem associated parenchyma cells (Collu, Garcia, Van der Heijden, & Verpoorte, 2002) associated with the lead vasculature. The assembly of geraniol begins within IPAP cells mediated by the plastid-localized geraniol synthase (Simkin et al., 2013). After export of geraniol to the cytosol of IPAP cells, it is oxidized to 10-hydroxygeraniol by the enzyme geraniol 10-hydroxylase (Fig. 1) (G10H; CYP76B6) to form 10-hydroxygeraniol (Burlat, Oudin, Courtois, Rideau, & St-Pierre, 2004; Collu et al., 2001; Collu et al., 2002; Meehan & Coscia, 1973; Suttipanta et al., 2007). The 10-hydroxygeraniol, in turn, is oxidized by 10-hydroxygeraniol oxidase (10HGO) to the aldehyde 10-oxogeraniol (Geu-Flores et al., 2012). This is followed by iridoid synthase (IS) converting the aldehyde to iridodial through cyclization, (Geu-Flores et al., 2012) and oxidized by 7DLS to form deoxyloganetic acid (Salim, Wiens, Masada-Atsumi, Yu, & De Luca, 2014)

The deoxyloganetic acid is glucosylated by the enzyme UDP deoxyloganetic acid-glycosyltransferase (UGT8) to form 7-deoxyloganic acid (Asada et al., 2013) and loganic acid is formed from the hydroxylation of 7-deoxyloganic acid mediated by 7-deoxyloganic acid-7-hydroxylase (DL7H) (Asada et al., 2013; Salim et al., 2014). The formation of Loganic acid is followed by its export from IPAP cells by unknown transport mechanisms to the leaf epidermis where it is O-methylated by loganic acid O-methyltransferase (LAMT) to form loganin (Murata, Roepke, Gordon, & De Luca, 2008; Roepke et al., 2010), followed by cyclopentane ring cleavage mediated by secologanin synthase (SLS) to yield secologanin (Fig. 1) (Irmler et al., 2000).

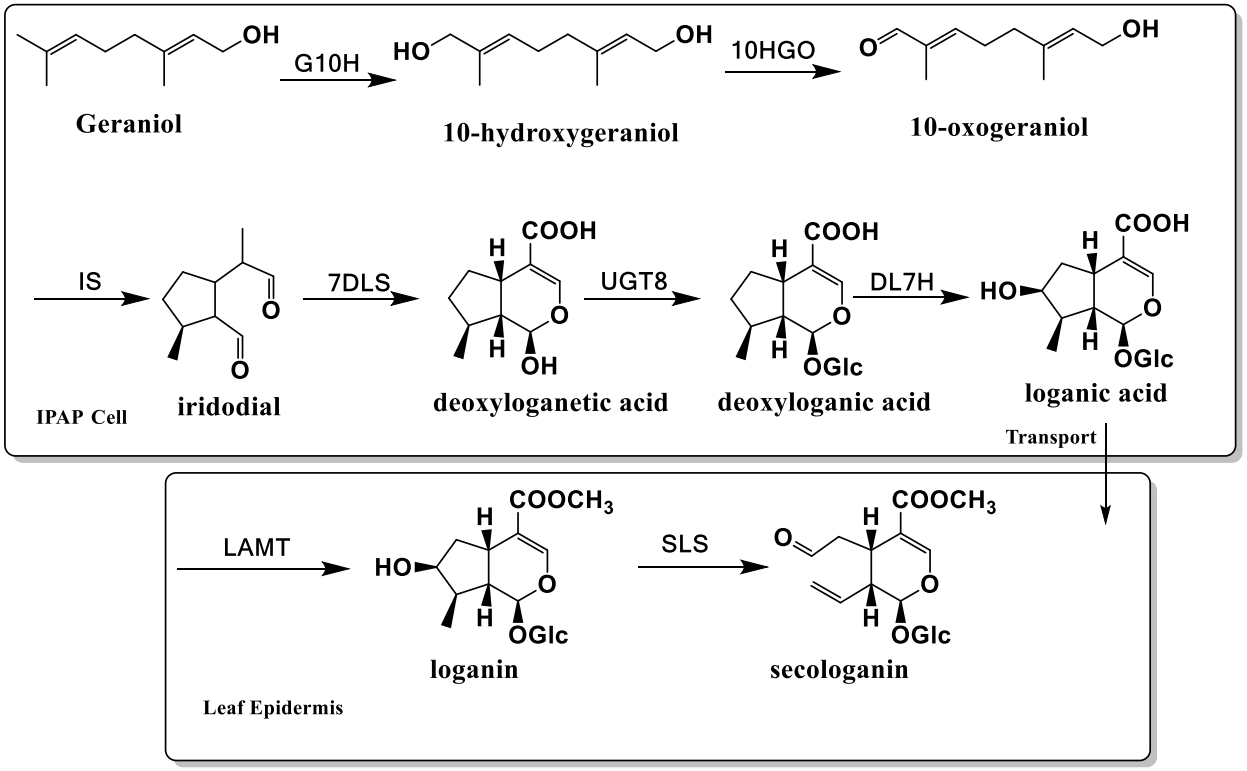

Figure 1: The biosynthesis of secologanin from geraniol involves leaf internal phloem associated parenchyma (IPAP) and leaf epidermal cells. The genes involved include geraniol 10-hydroxylase (G10H), 10-hydroxygeraniol oxidase (10HGO), iridoid synthase (IS), 7-deoxyloganic acid hydroxylase (7DLS), UDP deoxyloganetic acid-O-glycosyltransferase (UGT8), 7-deoxyloganic acid-7-hydroxylase (DL7H), loganic acid O-methyltransferase (LAMT) and secologanin synthase (SLS).

1.2.3 The mid-pathway: formation of strictosidine and labile intermediates required for the formation of different MIA backbones.

The first product in the mid pathway is strictosidine, the central MIA precursor, which is formed by adding an indole moiety from tryptophan (Fig. 2). Tryptophan, a product from the shikimic acid pathway, is decarboxylated by tryptophan decarboxylase to produce tryptamine (De Luca, Marineau, & Brisson, 1989). Tryptamine is combined with the product of iridoid biosynthesis, secologanin, to form strictosidine using the enzyme strictosidine synthase (STR) (De Luca et al., 1989). That coupling is a stereoselective Pictet-Spengler condensation of the two metabolites (Kutchan, 1989).

Next, Strictosidine-β-glucosidase (SGD) cleaves the sugar moiety on the central precursor strictosidine with this deglycosylation resulting in many unstable intermediates that form all the various MIAs. *Catharanthus roseus* cell cultures allowed the isolation and purification of SGD (Luijendijk, Stevens, & Verpoorte, 1998), followed by its cloning and functionally characterization (Geerlings, Ibañez, Memelink, Van Der Heijden, & Verpoorte, 2000). SGD is encoded by a single gene, and while it was first localized to the endoplasmic reticulum, subsequent research using yellow fluorescent protein tagging suggested it is also localized in the nucleus (Geerlings et al., 2000; Grégory Guirimand et al., 2010).

Deglycosylation of strictosidine results in a reactive hemiacetal intermediate which opens to form a dialdehyde which is further modified through the loss of the hydroxyl to form 4,21-dehydrocorynantheine aldehyde (Gerasimenko, Sheludko, Ma, & Stöckigt, 2002; O'Connor & Maresh, 2006). The resulting aldehyde is then rearranged to different strictosidine aglycones yielding the main classifications of MIAs in *C. roseus*: aspidosperma, corynanthe, and iboga.

The formation of ajmalicine from strictosidine aglycones has not been fully characterized. Carbinolamine is an intermediate to cathenamine, with the latter forming a reduction to result in ajmalicine. Cathenamine reductase (CR) uses cathenamine as substrate and NADPH as a cofactor, yielding ajmalicine and 19-epi-ajmalicine (El-Sayed & Verpoorte, 2007).

It is currently hypothesized that formation of iboga MIAs, such as catharanthine, and aspidosperma MIAs, such as tabersonine involves several enzymes that involve the formation of 4,21-dehydrogeissoschizine, preakummicine and stemmadenine intermediates (El-Sayed & Verpoorte, 2007; O'Connor & Maresh, 2006). However, this multienzyme pathway remains to be characterized at the biochemical and molecular level.

1.2.4 The late pathway in MIA biosynthesis

Vindoline, which is found solely in the shoot system and not in the roots of cell cultures, is along with catharanthine, one of the monomers bisindole alkaloid vinblastine (Fig. 2), is derived from the intermediate tabersonine through a seven step process which has just recently been elucidated (Qu et al., 2015). In the initial step, tabersonine is hydroxylated at the C-16 position by tabersonine 16-hydroxlase (T16H) which is yet another cytochrome P450 monooxygenase. This T16H step was first detected and characterized by (St-Pierre & De Luca, 1995) using total protein extracts from *C. roseus* leaves. T16H enzyme activity was found to be significantly lower in roots, stems, and older leaves, and the hydroxylase activity was dependent on NADPH.

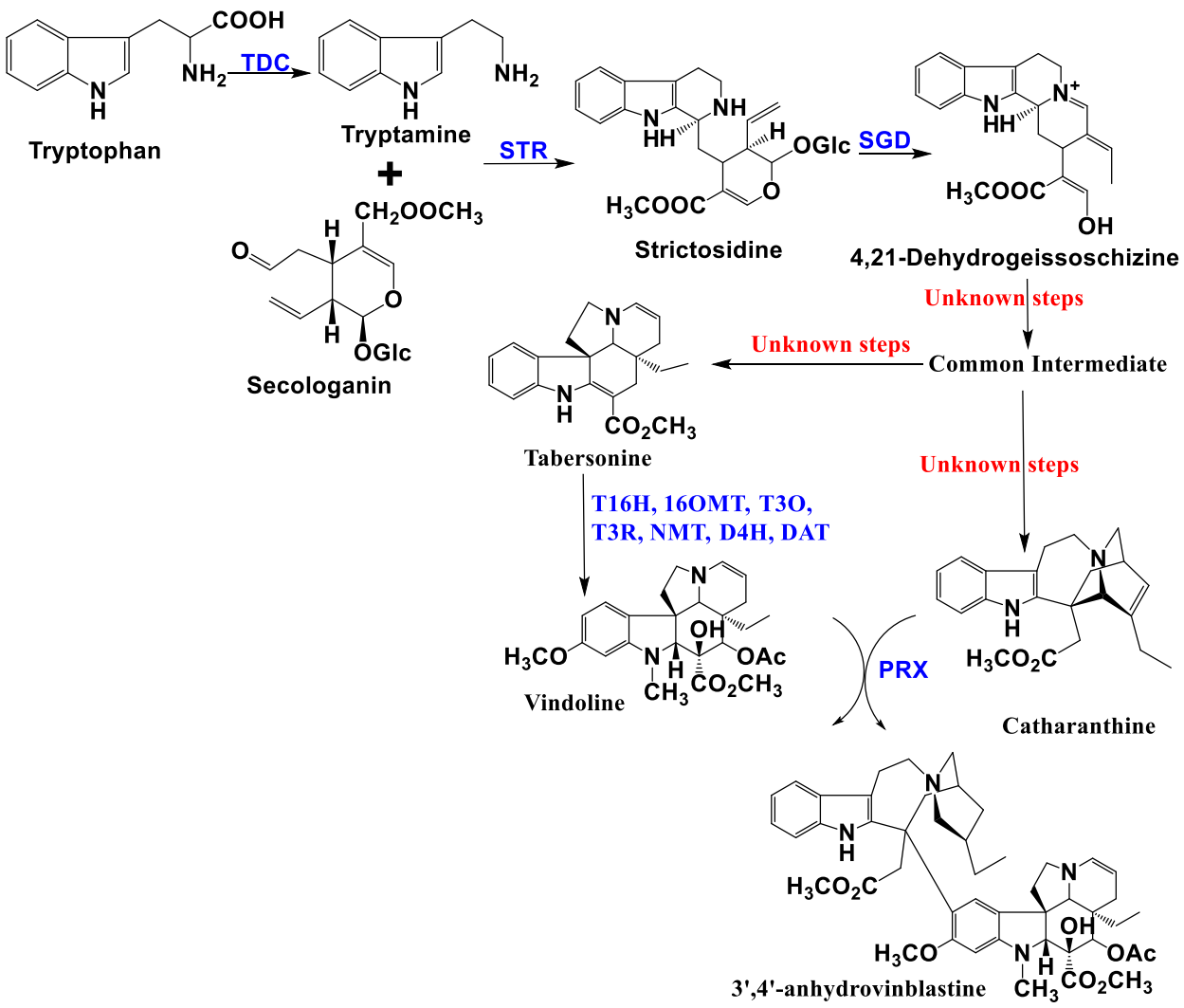

Figure 2: The biosynthesis of 3′,4′-anhydrovinblastine from L-tryptophan and secologanin. The known pathway genes include tryptophan decarboxylase (TDC), strictosidine synthase (STR), strictosidine β-glucosidase (SGD), tabersonine 16-hydroxylase (T16H), 16-hydroxytabersonine-16-O-methyltransferase (16OMT), tabersonine 3-oxidase (T3O), tabersonine 3-reductase (T3R), 16-methoxy-2,3-dihydro-3-hydroxytabersonine N-methyltransferase (NMT), deacetoxyvindoline 4-hydroxylase (D4H and acetyl-CoA deacetylvindoline O-acetyltransferase (DAT)

Next, the hydroxyl moiety is O-methylated by 16-hydroxy-tabersonine 16-O-methyltransferase requiring SAM co-substrate, to produce 16-methoxytabersonine (St-Pierre & De Luca, 1995). The first two enzymes in this pathway can be found in cell cultures, whereas the remaining three enzymes are only found in leaf tissues (St-Pierre & De Luca, 1995).

The third step converts the resulting 16-methoxytabersonine to 16-methoxy-2,3-dihydro-3-hydroxytabersonine (Kutchan, 1989) by the enzymes tabersonine 3-oxidase (T3O) and tabersonine 3-reductase (T3R) (Qu et al., 2015).

That product is further N-methylated to produce deacetoxyvindoline (16-methoxy-2,3-dihydro-3-hydroxy-N-methyltabersonine). The N-methyltransferase was localized to the thylakoid membrane (De Luca, Balsevich, Tyler, & Kurz, 1987) and the enzyme was cloned and functionally characterized by Liscombe, Usera, and O'Connor (2010). The enzyme has high substrate specificity with the absence of the 3-hydroxy group resulting in significantly lower N-methylation than with natural substrate (De Luca et al., 1987).

In the fifth step, deacetoxyvindoline is hydroxylated by 2-oxoglutarate-dependent dioxygenase, deacetoxyvindoline 4-hydroxylase (D4H) (De Carolis & De Luca, 1993; De Carolis et al., 1990; Vazquez-Flota et al., 1997) an enzyme that was purified and characterized by De Carolis and De Luca (1994).

The last step in vindoline biosynthesis (Fig. 2) involves the catalyzation of deacetylvindoline by acetyl-CoA deacetylvindoline O-acetyltransferase (DAT) (De Luca et al., 1987; St-Pierre et al., 1998) The enzyme is only in vindoline producing parts of the plant such as leaves, but not the roots.

1.3 Regulation of MIA biosynthesis

Studies have shown that MIA biosynthesis can be stimulated by treatment with the plant hormones cytokinins, ethylene, jasmonate, and methyl jasmonate while auxins 2,4-D, 1-Napthaleneacetic acid (NAA) and indole-3-acetic acid (IAA) reduce MIA biosynthesis (Zhu, Wang, Wen, & Yu, 2015).

2,4-D has been shown to strongly inhibit the expression of DXS, DXR and TDC genes in *C. roseus* cell suspension cultures, inhibiting MIA production in the process. NAA and IAA also downregulate TDC expression levels (Zhu et al., 2015).

Cytokinins and ethylene regulate steps in the MEP pathway and G10H gene expression levels, but only in the absence of auxins (Papon et al., 2005). In the case of cytokinins, the Ca^{2+}-calmodulin system seems to play a role (Verpoorte, van der Heijden, & Moreno, 1997). Jasmonates have multiple roles including plant signaling involved in the protection against pathogens and insects. Hairy root cultures have found that jasmonic acid treatment increases expression along the indole alkaloid pathway and results in an increased accumulation of ajmalicine, serpentine, lochnericine, and horhammericine (Zhu et al., 2015).

Methyl jasmonate (MeJA) is a signaling molecule that activates ORCA3, a jasmonate-responsive APETALA2 (AP2)-domain transcription factor gene which increases in transcript expression level of D4H, G10H STR, TDC, and cytochrome P-450 reductase (Zhu et al., 2015).

BIS1, a jasmonate-regulated basic Helix-Loop-Helix (bHLH) transcription factor found predominantly in IPAP containing tissues, and complementary to, but distinct from ORCA3, transactivates all of the genes in the iridoid pathway from geraniol synthase to 7-deoxyloganic acid hydroxylase, but not LAMT (Van Moerkercke et al., 2015). BIS1 overexpression in hairy roots did not lead to an increase in MIA production but interestingly did lead to an increase in

gene transcripts for the MEP and early iridoid pathway genes. At the same time, expression of LAMT, SLS, TDC and SGD genes were diminished (Van Moerkercke et al., 2015), and this latter decrease may explain why overexpression of BIS1 did not affect MIA levels. Attempts to silence BIS1 in *C. roseus* leaves using virus-induced gene silencing (VIGS) did not change MIA levels, but transformed *C. roseus* hairy roots with silenced BIS1 accumulated significantly lower levels of MIAs (Van Moerkercke et al., 2015).

The same group discovered a gene homologous to BIS1, BIS2, a jasmonate-responsive bHLH transcription factor. This gene activates the same MEP and early iridoid genes. However, when BIS2 is silenced, upregulation of those genes does not occur even with over-expression of BIS1. Ectopic expression of BIS1 was found to increase transcript levels of BIS1 and BIS2, while ectopic expression of BIS2 was found to increase transcript levels of only BIS2. It has been proposed that the transcription factor BIS2 is crucial for MIA production in *C. roseus* (Van Moerkercke et al., 2016).

1.4 Intercellular and intracellular transport of iridoid and MIAs

Alkaloid transport can be inter-organ, intercellular or intracellular (Shitan et al., 2014a). Three different mechanisms, which all are known to occur in plant cells, have been suggested for alkaloid transport. The first mechanism is simple diffusion followed by membrane trapping. Because alkaloids are weakly basic it is proposed that they, or at least some alkaloids, may be able to enter the tonoplast through simple diffusion (Shitan et al., 2014b). The second mechanism that has been suggested is a vesicle-mediated transport model for which small vesicles containing alkaloids have been observed using microscopy (Shitan et al., 2014b). The final mechanism is transporter-mediated membrane transport for which several vacuolar alkaloid

transporters have been identified and will be discussed in the upcoming paragraphs (Shitan et al., 2014b).

Three main families of transporters have been reported for alkaloids: ATP-binding cassette proteins, multidrug and toxic compound extrusion (MATE), and purine permease (PUP) families.

It is well understood that various steps within the biosynthetic pathways of MIAs occur in different cell compartments suggesting the transport of products of intermediates (Facchini & De Luca, 2008). Some of these movements have been discussed in the preceding paragraphs.

We know that the MEP genes and the early iridoid pathway genes are associated with the IPAP cells however, the LAMT and SLS genes have been localized to the epidermal cells via RNA in situ hybridization (Guirimand et al., 2011) suggesting that an unknown loganic acid transporter may transport loganic acid to the epidermis before conversion to secologanin. We also know that catharanthine is transported to the leaf surface by a characterized ATP-binding cassette (ABC) transporter (Yu & De Luca, 2013). However, as of yet no solid evidence exists for long distance transport of MIAs or pre-MIAs in *C. roseus*. While there is evidence for long distance transport including evidence for the long distance transport of alkaloids via both the phloem through which transport of quinolizidine, pyrrolizidine and indolizidine alkaloids has been demonstrated and xylem for which nicotine and berberine (*Coptis japonica*) alkaloids have been demonstrated, only nicotine transport has been significantly studied (Kehr, 2009).

Most Nicotiana species accumulate nicotine in undamaged leaves at a range of 0.1 – 1.0% of dry weight. After folivory, real or simulated, nicotine concentrations in the leaves

increase four- to tenfold, reaching levels that have been found to ward off insect herbivory (Baldwin, Sims, & Kean, 1990).

Experimental results consistently show that nicotine is synthesized in the roots and then transported within the xylem to the shoots. Dawson (1941) used grafting experiments combining the roots and shoots of nicotine-producing and non-nicotine producing tobacco species to show that only grafts with nicotine producing roots resulted in nicotine accumulation in the leaves. While it was known that damage to leaves increases nicotine concentration, it was not until 1994 that it was shown that leaf damage increases jasmonic acid pools and in turn increases the nicotine volumes within the roots, xylem and leaves (Baldwin et al., 1990).

Nicotine biosynthesis being reserved to within the roots means that physiologically there is a large gap between the site of synthesis and the site of damage from herbivore attack. This requires both a long-distance signal transduction pathway and a long-distance transport pathway from the newly synthesized nicotine to travel along.

Upon damage, the signal that is sent from the shoots to the roots travels through the phloem. The signal can be blocked by steam girdling to the stem below the site of damage. As steam kills the phloem but does not affect the xylem, this supports the evidence for the signal traveling through the phloem (Baldwin, Schmelz, & Ohnmeiss, 1994). The signal is slow moving taking hours for nicotine biosynthesis to begin, dismissing the possibility of an electrical signal (Baldwin et al., 1994).

Jasmonic acid, synthesized through the octadecanoid pathway (Howe & Jander, 2008), is known to be involved in the signal transduction cascade with the pools of jasmonic acid in the leaves increasing to its maximal value within 90 minutes of the leaf damage event. Jasmonic acid

levels also increase in the roots, reaching its highest values within 3 hours (Baldwin et al., 1994). It has also been demonstrated that the more extensively a leaf is wounded, the larger the jasmonic acid pool and the larger the increase in whole plant nicotine levels (Baldwin et al., 1997).

The role of jasmonic acid in the signal-transduction cascade is further supported by studies that show that jasmonate mutants are unable to resist a large range of herbivores that their wild-type relatives can easily fend off (Howe & Jander, 2008).

Two of the three transporter families for which there is evidence of alkaloid transport have been shown to transport nicotine. The two are the multidrug and toxic compound extrusion (MATE) family, and the purine uptake permease (PUP) family. Despite being a common alkaloid transporter, the ATP-binding cassette (ABC) protein family, has not been found to be involved in nicotine transport at this time (Shitan et al., 2014a).

MATE transporters received their name as they were first identified in *Vibrio parahaemolyticus* bacteria as transporters required for resistance to multiple drugs including the popular antimicrobial compound norfloxacin (Morita et al., 1998). They are antiporter membrane proteins that consist of about 500 amino acids with 9 – 12 transmembrane alpha-helices (Omote et al., 2006). In the years after the initial discovery other MATE transporters, often with the role of detoxification, were found in mammals, including two genes, MATE1 and MATE2, in humans, other animals, and plants (Shitan et al., 2014). For instance, AtDTX1 is one of 56 MATE transporters found in Arabidopsis. It facilitates the efflux of berberine and palmatine (Li, He, Pandey, Tsuchiya, & Luan, 2002). While most MATE transporters appear to accept a large range of substrates, others have limited substrate specificities (Shitan et al., 2014). MATE

transporters are also known to be involved in other physiological functions including the translocation of iron and plant hormone signaling (Shitan et al., 2014).

Nt-JAT1 (jasmonate-inducible alkaloid transporter 1) was first identified as a gene which encodes a MATE transporter through transcriptome analysis for genes up-regulated by MeJA. It is expressed throughout the entire plant, and it localizes to the tonoplast of leaf cells, transporting nicotine across that membrane (Morita et al., 2009). While Nt-JAT1 acts as an antiporter in the leaves translocating nicotine into the vacuoles, in the root cells it is localized to the plasma membrane where it is hypothesized that it may play a role in the efflux of nicotine from the root cells to the xylem (Shitan, Hayashida, & Yazaki, 2015).

More recently the Nt-JAT2 MATE transporter was isolated. It also localizes to the tonoplast in leaves, transports nicotine, and is induced by MeJA treatment. However, unlike Nt-JAT1 which is found throughout the plant, Nt-JAT2 is solely expressed in the leaves. Like Nt-JAT1, JAT2 may play a role in the protection of leaves from insect attack by increasing the volume of nicotine in the vacuoles (Shitan et al., 2015).

Two other transporters in tobacco are NtMATE1 and NtMATE2 which have an amino acid sequence identity of 96%. These are both found almost exclusively in the roots where nicotine is not just synthesized, but also accumulates in the vacuoles, where both of these MATE transporters play a role (Shoji et al., 2009). This is supported by a study using GFP-fusion proteins and immunogold electron microscopy which found that NtMATE1 and NtMATE2 were both localized to the tonoplast (Shoji et al., 2009). Further evidence was supplied by a nic1nic2 regulatory mutant with a low nicotine phenotype which also showed down-regulation of both NtMATE genes (Shitan et al., 2014; Shoji et al., 2009). All four MATE transporters are rapidly induced by MeJA treatment (Shitan et al., 2015).

In addition to the four known MATE transporters, there is a fifth nicotine transporter, from the PUP transporter family, called nicotine uptake permease 1 (NUP1). This transporter is expressed mainly in root tips; the site where nicotine biosynthesis is most active. NUP1 is localized to the plasma membrane where it translocates nicotine into the root cells from the apoplast (Hildreth et al., 2011).

The transport of iridoid glucosides is found with both antirrhinoside and catalpol, both of which are transported within the phloem. Within *A. majus* the iridoid glucoside, antirrhinoside, is likely phloem mobile and is allocated constitutively at much higher concentrations in young leaves, buds, and flowers, reaching 20% of the dry weight of those tissues, whereas the lowest concentrations are found in the root tissue. While antirrhinoside is present in all tissues of *A. majus*, a second major iridoid antirrhide is found only in the leaves. The relative concentrations of these two iridoids change with time as the leaves age; antirrhinoside declines and the concentration of antirrhide increases (Beninger et al., 2008).

In *Asarina scandens*, antirrhinoside is a phloem-mobile compound. It has been hypothesized that the ability to transport antirrhinoside within the plant to growing sinks could function as a defense against herbivory. However, antirrhinoside may also play a role in plant osmoregulation. In *Asarina barclaiana*, antirrhinoside comprised 39% of the total carbon transported in the phloem. Apoplastic loading of this compound, as well as sucrose, could contribute to regulation of the osmotic pressure during long distance transport of assimilates (Beninger et al., 2007; Braun, Wang, & Ruan, 2014; Chen et al., 2012; Chen, Petersen, Olsen, Schulz, & Halkier, 2001).

Beninger et al. (2007) sought to determine whether or not it is likely that either of the major iridoids in *A. majus* is translocated within the plant through the use of 14C labeling

experiment on mature leaves. They found that the concentration of antirrhinoside and antirrhide was dependent on leaf position. Antirrhinoside levels were highest in the youngest leaves, decreased as the leaves aged, and were also found in the roots. Antirrhide levels were lowest in the youngest leaves, increased as the leaves aged, and was not found in the roots. As antirrhide is not found in nonleaf tissue, while antirrhinoside is, the former is probably not transported within the plant whereas the latter is (Beninger et al., 2008).

Catalpol, found in *Plantago lanceolata*, reduces the growth of *Spodoptera eridania* (Beninger, Cloutier, & Grodzinski, 2009). Younger leaves of *P. lanceolate* were found to have large amounts of catalpol, while older leaves had no iridoids. Aucubin, a precursor to catalpol, was found in high levels in older leaves, but not in the youngest leaves. It has been suggested that in young leaves aucubin is not found because it is rapidly converted to catalpol, however, in older leaves the conversion may become inefficient, or catalpol may be transported elsewhere (Beninger et al., 2007).

While it is known that these iridoid glycosides are transported in the phloem, little study has been done.

1.5 Conclusion and goals of study

While MIA biosynthesis has been extensively studied in *Catharanthus roseus*, much remains to be learned about the remaining steps involved in the assembly of tabersonine and catharanthine as well as the biochemistry and molecular biology of iridoid and MIA transport within and between cells within the organism. The major goal of this study is to use a trace MIA *Catharanthus roseus* mutant obtained through EMS mutagenesis to learn more about MIA biosynthesis and its regulation. The present study proposes to **i)** characterize its iridoid and MIA

profile in different plant organs in the mutant compared to the parental line (WT); **ii)** characterize the parts of iridoid and MIA biosynthesis that may be affected as a result of EMS mutagenesis; **iii)** investigate if iridoids and/or MIAs are transported between *C. roseus* organs.

2 Materials and Methods

2.1 Plant Material

In vitro sterile cultivation of the *Catharanthus roseus* mutant (M2-1582)

The *Catharanthus roseus* mutant (M2-1582) was highly susceptible to fungal infection when cultivated in the greenhouse and would have died if it had not been rescued by cultivation under *in vitro* sterile conditions. *In vitro* culture of M2-1582 was successfully achieved by PhD student Paulo Cazares, who harvested nodes from the infected plant, washed them with sterile water, submerged them in 70% ethanol for 2 minutes and in 20% bleach for 10 minutes. The nodes were then washed 5 times with sterile water and placed in a sterile magenta box containing plant regenerating media composed of autoclaved Woody plant medium salts (2.3g/L), indole butyric acid (0.2 mg/L), glycine (2.0 mg/L), myo-inositol (100 mg/L), nicotinic acid (0.5 mg/L), pyridoxine (0.5 mg/L), thiamine-HCl (0.1 mg/L) and sucrose (30 g/L), activated charcoal (2.5 g/L), gelrite (2.6 g/L) adjusted to pH 5.8 with ~4 drops of 1M KOH.

In vitro sterile cultivation of the *Catharanthus roseus* variety Pacifica Peach

Catharanthus roseus variety Pacifica Peach seeds (ballseed.com) were sterilized with 70% ethanol for 2 minutes followed by a 20% bleach solution for 15 minutes. The seeds were then washed with sterile water six times and placed on filter paper in a petri dish for germination. Post-germination seedlings were transferred to magenta boxes containing the same media used to cultivate the M2-1582 mutant with Catharanthus growth -plantlets media. Propagation of the control line was performed by taking cuttings from a single individual plant and all experiments were performed using propagated material from this individual.

Re-introduction of *C. roseus* control and mutant plants to greenhouse cultivation.

The *Catharanthus roseus* control and mutant plants were transferred from *in vitro* cultivation to greenhouse cultivation after acclimation. All in vitro cultures were maintained at 21 °C in a culture room with a 16/8 hour photoperiod. Cuttings were made of the parental (WT) line every 3 to 6 weeks and for the mutant line every 8 to 12 weeks due to slower growth. While control plants were successfully cultivated in the greenhouse, all attempts to reintroduce the mutant were unsuccessful. Thus the mutant could only be maintained under sterile conditions and through propagation through cuttings.

Alkaloid extraction from plants.

Fresh first leaf pairs from the parental and mutant lines were harvested and their fresh weights were recorded. The surface alkaloid extracts were obtained from freshly harvested leaves which were dipped in 1 ml chloroform at room temperature for 1 hour. The chloroform extracts were dried under vacuum centrifugation in an SPD SpeedVac (Fisher Scientific) and resuspended in methanol according to leaf fresh weight (2 ml per 100 µg fresh weight). Once the surface alkaloids were stripped, internal cell alkaloids were obtained through air drying the leaves for 30 minutes in a fume hood and then frozen in liquid nitrogen, pulverized with a pestle and homogenized in methanol according to leaf fresh weight (2 ml per 100 µg fresh weight).

2.2 Chemicals

All reagents were purchased from Sigma-Aldrich (Oakville, Canada) in ≥90% purity unless otherwise stated. Secologanin was purchased from Sigma-Aldrich (Oakville, Canada). Loganin was obtained from Wako Pure Chemicals (Osaka, Japan). 7-Deoxyloganic acid was

prepared from 7-deoxyloganin tetraacetate as described by Salim (2013) and Nagatoshi et al. (2011). Loganic acid was obtained from Extrasynthese (Genay, France). The standard curves for Catharanthine (y=0.0394x), Vindoline (y=0.0155x+3.226), Secologanin (y=0.018x-19.925), 3',4'-Anhydrovinblastine (y=0.0286+10.567), 16-methoxytabersonine (y=0.0182+0.1555), Deacetylvindoline (y=0.0504+3.2245), Serpentine (y=0.0233x), Tabersonine (y=0.0106+3.8138), and Vindolidine (y=0.0155x+3.226) quantification were obtained from previous studies (Qu et al., 2015; V Salim, 2013). X represents peak area. Y is nanograms of alkaloid analyzed.

2.3 Grafting

After some experimentation with several methods, the Top Wedge Grafting method (Mudge, 2015) was used for all grafting. Experimentation also found that the stock plant was unable to support a scion with more than one leaf pair. A horizontal cut made with a scalpel was used to separate and remove the terminal portion of the stock plant. The scalpel was then used to split the stem of the stock plant, cutting vertically approximately 1 cm. The scion is cut horizontally around the second node, and then the lower 1 cm is tapered using the scalpel into a "V' shaped wedge. The scion is inserted into the stock, and grafting wax is applied to reduce desiccation and provide support.

As this grafting is performed on tissue culture plants, it is done in the laminar flow hood. Both the scion and stock plants are in magenta boxes. The cutting within a magenta box is not a problem for the scion material, but the stock must be cut in the right location to allow one set of tweezers to secure the stock while the second set of tweezers inserts the scion. I have found that the best height for the cut of the stock plant is at 4.0 to 4.5 cm from the top of the box.

The stem of the mutant line is more rigid than the stem of the parental line. This results in the parental line being more difficult as a stock.

2.4 Feeding Experiments

Several feeding experiments were attempted. Mature plants, both parental line, and mutant were transferred from the magenta box to 50 ml falcon tubes with 3 – 5 ml of fluid with MS for the control and the control fluid plus the addition of 1 mM of either secologanin, loganin, loganic acid or 7-deoxyloganic acid. Leaves were removed after 0 hrs, 24 hrs and 48 hrs for alkaloid and iridoid analysis.

2.5 UPLC-MS Analysis

A Waters Ultra Performance Liquid Chromatography and Mass Spectrometry system (UPLC-MS) was used to separate and identify alkaloids. Analytes were separated using an Aquity UPLC BEH C18 column with particle size 1.7 µm and dimensions of 1.0-50 mm. The solvent systems for alkaloid analysis were set as follows: Solvent A- methanol: acetonitrile: 5 mM ammonium acetate (6:14:80) and Solvent B- methanol: acetonitrile: 5 mM ammonium acetate (25:65:10). The linear elution gradient which was used by the system was set up as follows: 0 – 0.5 min 99% A, 1% B at 0.3 mL/min; 0.5-0.6 min 99% A, 1% B at 0.4 mL/min; 0.6-7.0 min 1% A, 99% B at 0.4 mL/min; 7.0-8.0 min 1% A, 99% B at 0.4 mL/min; 8.0-8.3 min 99% A, 1% B at 0.4 mL/min; 8.3-8.5 min 99% A, 1% B at 0.3 mL/min; 8.5-10.0 min 99% A, 1% B at 0.3 mL/min. The mass spectrometer capillary voltage was operated at a potential of 3.10 kV, cone voltage of 48 V, cone gas flow of 1 L/h, desolvation gas flow of 600 L/h desolvation temperature of 350 °C and a source temperature of 150 °C. Alkaloids were additionally detected by a photodiode array at 280 nm or 305 nm.

For iridoids, phenolic analyses were set up as solvent system with 0.1% formic acid in water (solvent A) and 0.1% formic acid in acetonitrile (solvent B). The elution gradient was as follows: 0-0.5 min 99% A, 1% B at 0.3 mL/min; 0.5-5 min 92% A, 8% B at 0.3 mL/min (curve 5); 5-6.5 min 70% A, 30% B at 0.3 mL/min (curve 7); 6.5-7.2 min 50% A, 50% B at 0.3 mL/min (curve 6); 7.2-7.5 min 70% A, 30% B at 0.3 mL/min (curve 6); 7.5-8.0 min 92% A, 8% B at 0.3 mL/min (curve 6) and 8.0 min 99% A, 1% B at 0.3 mL/min (curve 6). The mass spectrometer capillary voltage was operated at a potential of 3.50 kV, cone voltage of -50V, cone gas flow of 1 L/h, desolvation gas flow of 600 L/h, desolvation temperature of 350 °C, and source temperature of 150 °C. Phenolic compounds were analyzed in negative electron ion spray mode. Secologanin was detected by a photodiode array at 240 nm.

2.6 RNA extraction and cDNA synthesis

Each leaf (leaf pair 1, leaf pair 2 or leaf pair 3, for a range of leaf maturity) stem and root was ground in liquid nitrogen to a fine powder and immediately mixed with 0.8 mL of Trizol® reagent (Life Technologies) to extract the RNA. RNA was isolated according to manufacturer's protocol. Briefly, after extraction of RNA with Trizol, 0.16 mL of chloroform was added, the aqueous phase was removed. After precipitation with 0.4 mL of isopropanol and 0.8 mL of ethanol, the RNA was suspended in 25 µl of DEPC H_2O. The RNA was subsequently treated with DNAase I to remove genomic DNA. DNAase I was in turn inactivated with 1 mM EDTA for 15 min at 75C. Quality and quantity of RNA were determined visually by gel electrophoresis as well as by nanophotometry before proceeding to cDNA synthesis. First-strand cDNA was synthesized using SuperScript II reverse transcriptase (Invitrogen, Carlsbad, CA) and oligo (dT) 12-18 primer (Invitrogen, Carlsbad, CA) using 1-4 µg total RNA according to manufacturer's protocol.

2.7 Quantitative Real-time PCR for iridoid expression analysis

qRT-PCR was performed (CFX96™ Real-Time system, Bio-Rad, Hercules, CA and CFX96 Connect™ Real-Time system, Bio-Rad, Hercules, CA) using 5 µL iTaq™ Universal SYBR® Green Supermix (Bio-Rad, Hercules, CA) 0.25 µL primer and cDNA template at 5 ng total RNA per 10 µL reaction volume.

The reaction conditions for qRT-PCR included 1 cycle of 95C for 1 min and 40 cycles of 95C for 15s and 58C for 1 min. Critical Threshold (Ct) values were used to calculate the relative transcript abundance with the housekeeping gene 60S ribosome RNA as the internal control.

Expression levels of each target gene were analyzed with the Bio-Rad CFX Manager Software (Bio-Rad) and normalized to the 60S ribosomal housekeeping gene.

Table 1 - List of primers used for iridoid expression analysis

Name	Sequence	Name	Sequence
G10H-F	GGTAGCCTCACGATGGAGAA	**G10H-R**	CCTTGGCAGAATCCGAATAA
10HGO-F	GTCTTGGTGGTCTTGGCCATG	**10HGO-R**	CTAACCAAGAAAGAATCAGCACC
8HGO-F	CGAATGCACTGGAGTTCCAGCTTT	**8HGO-R**	AAGTCCTGCCCCAATCAATACTGC
SLS-F	CTTGAGGGGTGCAAAATGGT	**SLS-R**	TGGGATCCTTGTTTTTCAGC
LAMT-F	ACTGGTGCTGGTTTGCTTCACT	**LAMT-R**	GGCAATTCCATCAAGGAAGTTCCCA
7DLS-F	GAAACCCACACGCATTCAAG	**7DLS-R**	GCAAATTCTCCATGTCGCTC
DLGT-F	GATGGGGTTTTGAGCTTTGC	**DLGT-R**	AGCCCAGAAAGAACAAGCAG
STR-F	CCAAGATGGCCGAGTTATCA	**STR-R**	TTTTCTCTGGATCGGTGCTG
TDC-F	TAAGACTGGCTGTTGGCTCATCG	**TDC-R**	TCCCAAACACGGCGTACATGAT
SGD-F	ATTTGCACCAGGAAGAGGTG	**SGD-R**	TATGAACCATCCGAGCTGA
BIS1-F	GCATTCACTCCAACAGCCGAATCT	**BIS1-R**	AAGGAAGTTCCGTAGCCAATGCAC
BIS2-F	GGCTCAATCTTGGCGTTACCAACA	**BIS2-R**	CCAAGAGCCAAGCTTCCAAATGGTG
***P5βR1*-F**	GGGCCGTAAGAAAAATTCGAATTTG	***P5βR1*-R**	GGAAGGATCTCGGCCAGGCTATTA
***P5βR2*-F**	CCTTCCATCCGTTCATCAATTTG	***P5βR2*-R**	GGGTGATCAAAATCATCCAATTT
***P5βR3*-F**	ACAGATATGGGCAGCATTGATCATCTTC	***P5βR3*-R**	TTCTCCCCATCAAATTCAACAAACTCCA
***P5βR4*-F**	GGAACACTGCAAAATCACTTGT	***P5βR4*-R**	ATTCCAAGAACCGCCAAAATGA
***P5βR5*-F**	TCTTGGGTTTTAGGAATTCGATGA	***P5βR5*-R**	AAACCAAACCCAAAGCAGAAAA
***P5βR6*-F**	TTTGAGCTTGAATTGCCATTTGATGA	***P5βR6*-R**	GTGCAAAATAAGTGCAATGCCTCAAA

3. Results

3.1 Screening and identification of a trace MIA mutant (M2-1582)

The cultivation and chemical screening of 3000 ethyl methane sulphonate (EMS) mutagenized *Catharanthus roseus* plants was performed by undergraduate student Michael Easson who was funded by an NSERC Undergraduate Student Research Award in the summer of 2013. This chemical mutagen introduces an average of one mutation per 100,000 base pairs, and it has been used extensively in breeding programs to create desirable phenotypes in crop plants (Section 1.1.1). The screen of MIA mutants involved a simple screen where *C. roseus* leaves were dipped in chloroform in order to harvest MIAs secreted to the leaf surface, followed by methanol extractions of leaves to harvest alkaloids found within the leaf. Samples were dried by vacuum centrifugation and suspended in a small amount of methanol in preparation for screening by silica gel thin layer chromatography (TLC). After TLC, the plates were exposed to short (252 nm) and long (365 nm) wave ultraviolet light to visualize MIAs and were documented by photography. This method allowed the screening of 250-300 plants per week and led to the successful identification of 3 MIA mutants. Two mutants produced little or no MIAs, while another mutant contained low levels of vindoline and accumulated new unidentified MIAs. Unfortunately, both low MIA lines were highly susceptible to fungal infection, and only one line (M2-1582) could be rescued by cultivating it in under sterile *in vitro* conditions (Section 2.1).

3.2 The M2-1582 line shows several abnormal growth characteristics compared to the parent line.

When the parental (*C. roseus* var. Pacifica Peach, WT) and mutant (M2-1582) lines were cultivated under *in vitro* conditions, several phenotypic differences were observed. The mutant line grew approximately eight times more slowly than the WT parent; it displayed premature

senescence (Fig. 3A), produced dense closely spaced leaves on short internodes (Fig. 3B) and produced a thick, stocky, short root system (Fig. 3C). More detailed analyses showed that WT leaf pairs 1, 2 and 3 (Fig. 4ACE) were 212, 336 and 287 % greater in fresh weight and were visually much larger than those of the mutant (Fig. 4BDE). Mutant leaves appeared to be more rigid and detached easily compared to those of WT. The stems of WT had longer internodes (Fig. 5A; 1.0 to 1.5 internodes/cm) compared to those of the mutant (Fig. 5B; 3.5 to 4.5 internodes/cm). The roots of WT were long and diffuse (Fig. 5C) compared to those of the mutant that formed a tightly twisted bundle that did not branch and extend out into the media (Fig. 5D). When comparing the fresh weight distributions of WT and Mutant plants (Table 2), the mutant root system represented 69.3 % of the plant fresh weight compared to only 16.5 % of the plant fresh weight in WT.

Apart from slow growth rates, these phenotypic features increased the difficulty and time required for propagating the mutant line compared WT and only 150 individual *in vitro* plants could be produced after eight months. Approximately 100 robustly growing *in vitro* WT plants were easily produced at the same time. With these numbers, adequate plant materials became available for further propagation of mutant and WT and for performing the experiments described in this thesis. Presently, the basis for these important phenotypic differences is not understood but may reflect a mutation that affects hormone-regulated processes that are responsible for this.

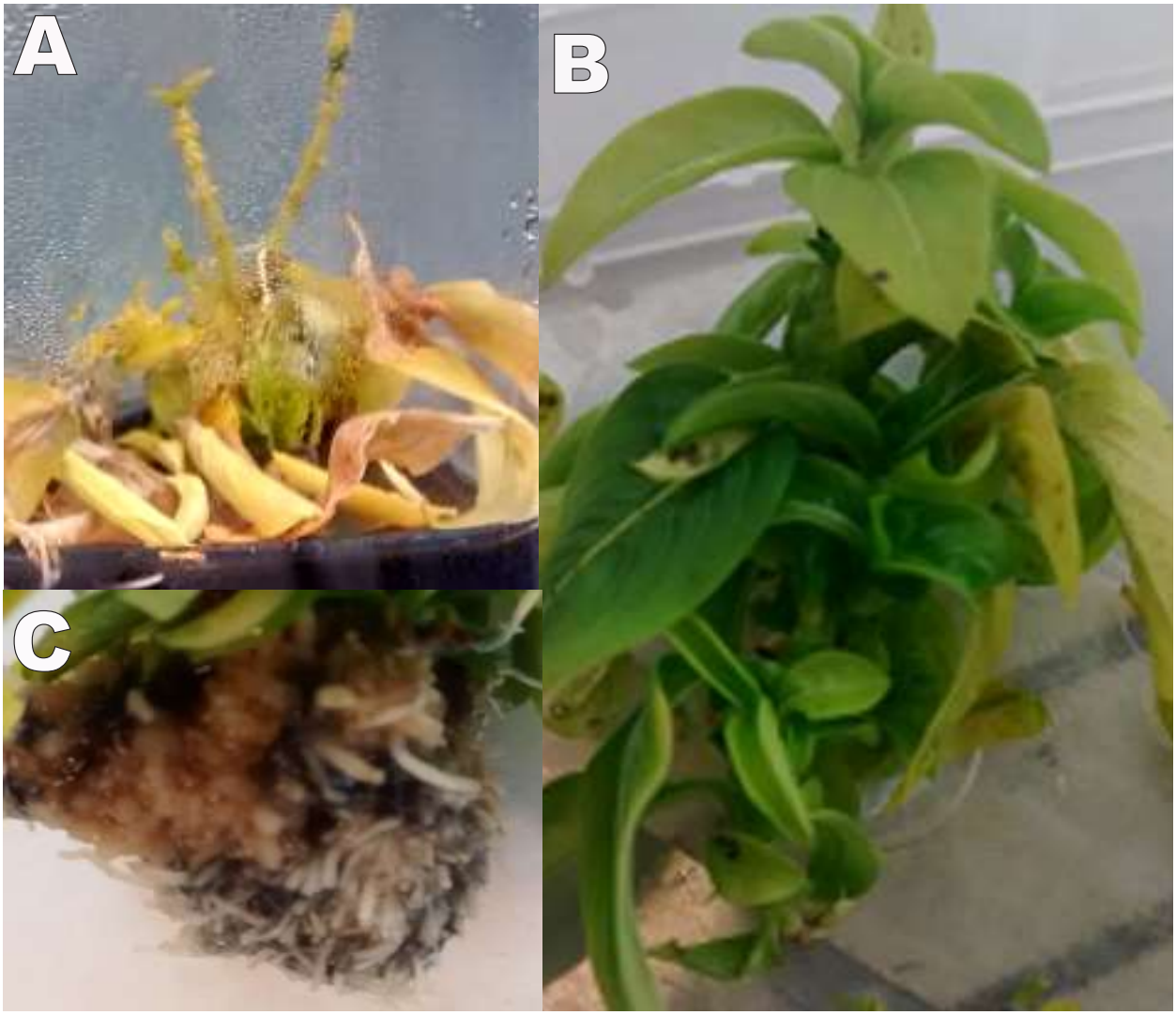

Figure 3: Line M2-1582 displays A) early senescence (24 weeks of cultivation); B) Dense closely packed leaves due to short internode growth; C) densely packed root growth compared with WT.

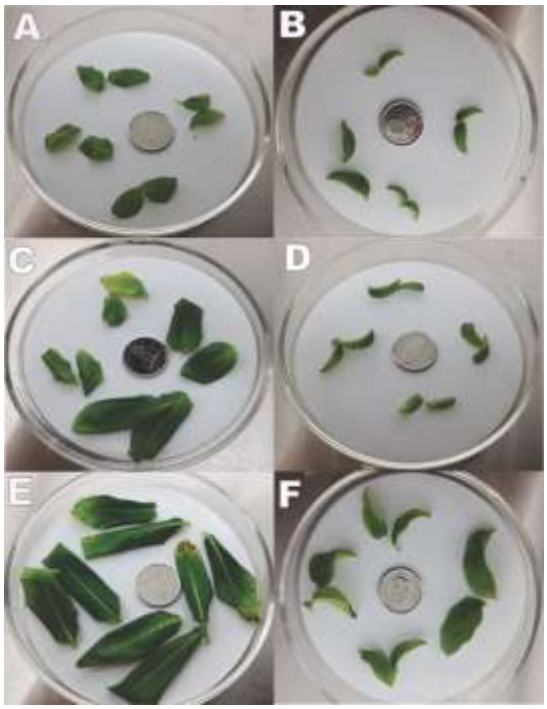

Figure 4: The leaves from WT are significantly larger than those from Line M2-1582. A) WT leaf pair one (average 18 mg/leaf); B: Mutant leaf pair one (8.5 mg/leaf); C: WT leaf pair two (average 37 mg/leaf); D: Mutant leaf pair two (11 mg/leaf); E: WT leaf pair three (89 mg/leaf); F: Mutant leaf pair three (31 mg/leaf).

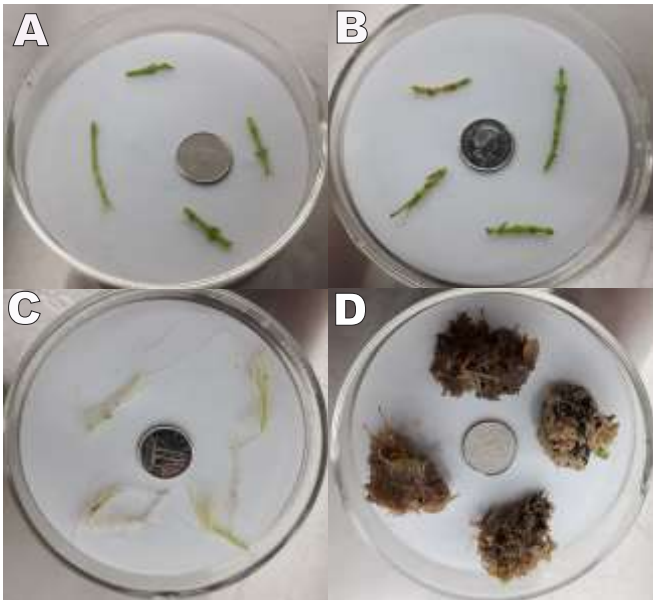

Figure 5: Line M2-1582 contains short internodes and roots formed into a tight twisted unbranched bundle that did not elongate compared to the WT. A: WT stems; B: Mutant stems; C: WT roots; D Mutant roots.

Table 2 – The root fresh weights of WT and M2-1582 lines show significant differences.

	WT Line (6 replicates)	Mutant Line (6 replicates)
Total fresh weight (g)	2.27 ± 0.38	2.21 ± 0.56
Shoot fresh weight (g)	1.89 ± 0.26	0.69 ± 0.17
Root fresh weight (g)	0.38 ± 0.11	1.52 ± 0.49
% of mass in roots	16.5%	69.3%

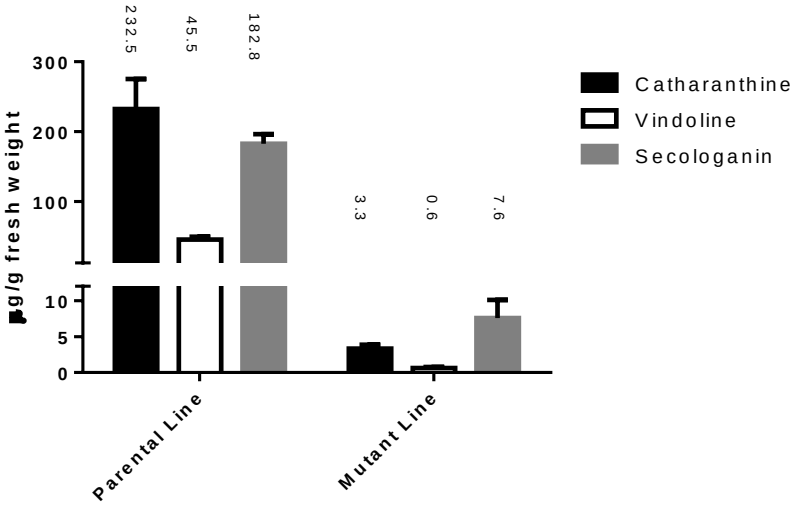

Figure 6: Line M2-1582 accumulates low MIAs compared to WT. The error bars represent the average of 5 biological replicates of catharanthine, vindoline, and secologanin UPLC-MS measurements.

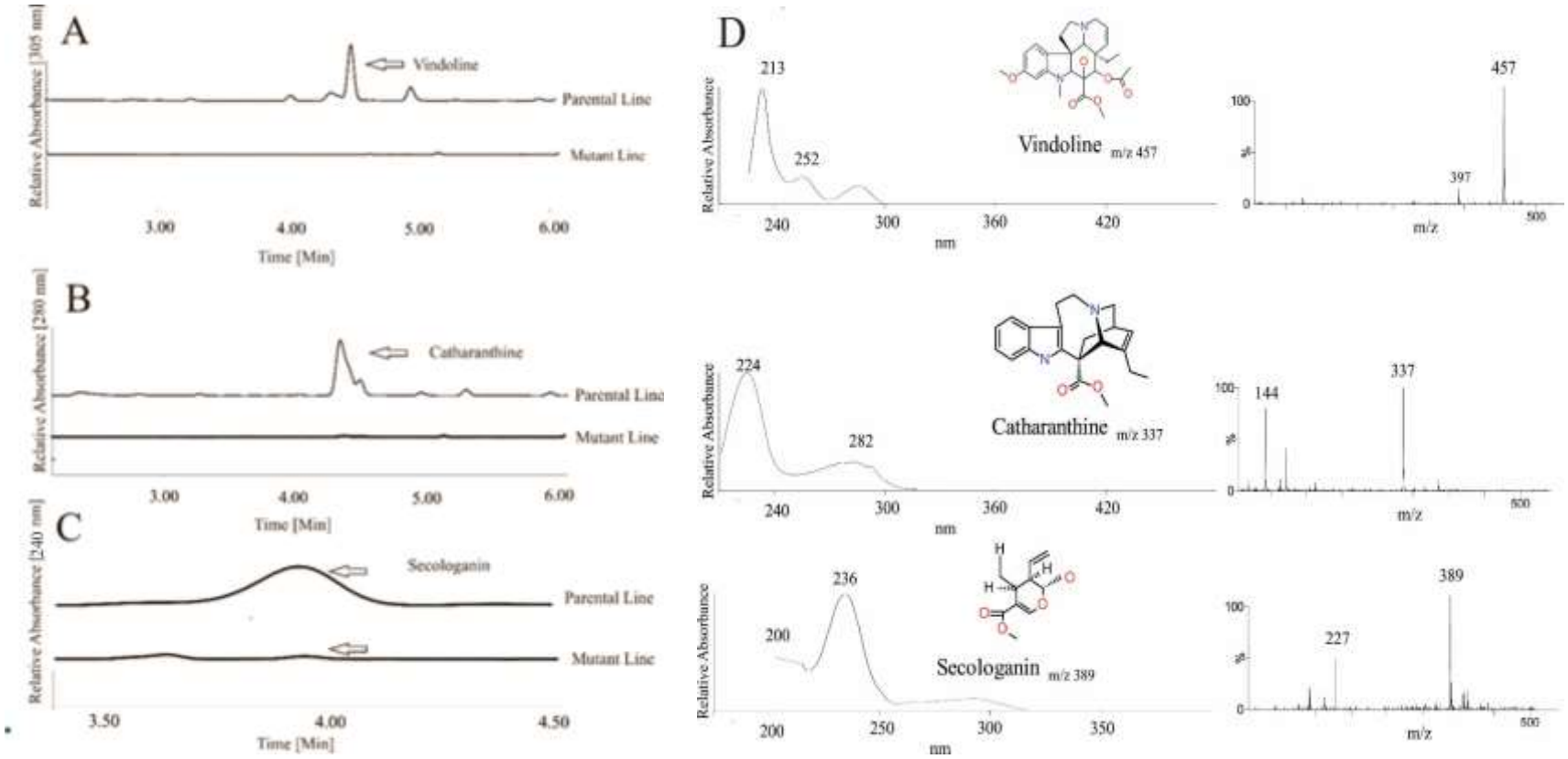

Figure 7: UPLC-MS show M2-1582 accumulates low MIAs compared to WT. UPLC-MS profiles of MIAs were measured at: A) 305 nm, at B) 280 nm, and at C) 240 nm to show elution of A) vindoline B) catharanthine, and C) secologanin detected at 240 nm disappeared in leaf pair 1 of the line M2-1582 compared to WT. D) shows MS data for vindoline, catharanthine, and secologanin.

3.3 M2-1582 contains almost no MIAs and iridoids.

Leaves harvested from the WT and M2-1582 were extracted and analyzed for the presence of the major MIAs, catharanthine, vindoline and the major iridoid, secologanin. Surprisingly, the mutant contained over 70-, 76- and 24-fold less of these end-products than the WT line (Fig. 6). Remarkably, other typical *C. roseus* MIAs and iridoids were not detected in the M2-1582 line. These results suggest that MIA levels may have dropped in the mutant because of some impediment in the biosynthesis of secologanin that is required for the assembly of all *C. roseus* MIAs.

3.4 Low secologanin and MIA levels in the M2-1582 line is caused by iridoid pathway down-regulation.

It has been proposed based on studies with *C. roseus* cell suspension and hairy root cultures, that the transcription factors BIS1 and/or BIS2 activate expression of 7 genes [geraniol synthase to 7-deoxyloganic acid hydroxylase (7DLS)] involved in secologanin biosynthesis (Van Moerkercke et al., 2016). Since secologanin levels were very low in the mutant, the relative expression of *C. roseus* iridoid pathway transcription factors and seven secologanin biosynthesis genes were monitored by real-time PCR (qPCR) using transcripts isolated from leaf pair 1. Remarkably, both *BIS1* and *BIS2* transcript levels were 3- and 13-fold lower in the M2-1582 line, respectively, than those of WT (Fig. 8). Depending on which reference is used, 10-hydroxygeraniol or 8-hydroxygeraniol represents the same product (IUPAC name (2E,6E)-2,6-dimethyl-2,6-octadiene-1,8-diol). The expression of geraniol 10-hydroxylase (*G10H*) and 10-hydroxygeraniol oxidoreductase (*10HGO*) were over 8- and 15-fold higher than in WT (Fig. 8). However, it has been suggested that *10HGO* might not actually be involved in iridoid

biosynthesis since its expression in IPAP cells was not demonstrated. In contrast, another gene named 8-hydroxygeraniol oxidoreductase (*8HGO*) (Miettinen et al., 2014) was suggested to be directly involved in iridoid biosynthesis. Since expression of *8HGO* declined almost 200-fold compared to those of WT, this provides evidence for this gene rather than *10HGO* being directly involved in precursor supply in the secologanin pathway.

Iridoid synthase (IS) (Geu-Flores et al., 2012), originally classified as a progesterone 5β – reductase, is part of a six-member family found in *C. roseus* (Munkert et al., 2015). *IS* declined almost 48-fold in line M2-1582 compared to WT, while the 4th member of this family (*CrP5βR4*), also declared to be a possible participant in this pathway (Munkert et al., 2015) declined over 6-fold (Fig. 9) while gene expression for the other 4 members of this gene family was relatively unaffected. Expression of 7-deoxyloganetic acid synthase (*7DLS*) and deoxyloganic acid glucosyltransferase (*DLGT*) declined 5- and 3-fold in line M2-1582, respectively, compared to WT. These results clearly suggested that the trace MIA phenotype of the mutant was likely caused by a mutation that prevents expression of *BIS1* and *BIS*2 that would normally activate multiple steps in iridoid biosynthesis (*8HGO, IS (CrP5βR4), 7DLS, DLGT*) (Munkert et al., 2015).

3.4.1 Expression of *LAMT, SLS, TDC, STR* and *SGD* are not down-regulated in line M2-1582.

LAMT and SLS that catalyze the last two steps in the assembly of secologanin are expressed in leaf epidermal cells (Guirimand et al., 2011), unlike all previous pathway steps that occur in IPAP cells. Previous studies with *BIS1* expressing hairy root cultures (Van Moerkercke et al., 2015) showed that expression of *LAMT, SLS, TDC* and *SGD* genes were suppressed. The 3-fold increase in *LAMT* and *SLS* expression (Fig. 8) observed in the *BIS1/BIS2* suppressed

mutant (Fig. 8) might have been expected based on the observed inhibitory effect of *BIS1* on the expression of these genes in hairy root cultures. While expression of *STR* was slightly decreased, expression of *SGD* and *TDC* were both increased 4-fold in the mutant compared to WT. Together these results provide significant insights on the different regulation patterns of IPAP localized parts of iridoid biosynthesis compared to the last two steps in iridoid biosynthesis by LAMT and SLS, the decarboxylation of tryptophan by TDC and in the assembly of strictosidine and downstream MIAs occurring in the leaf epidermis.

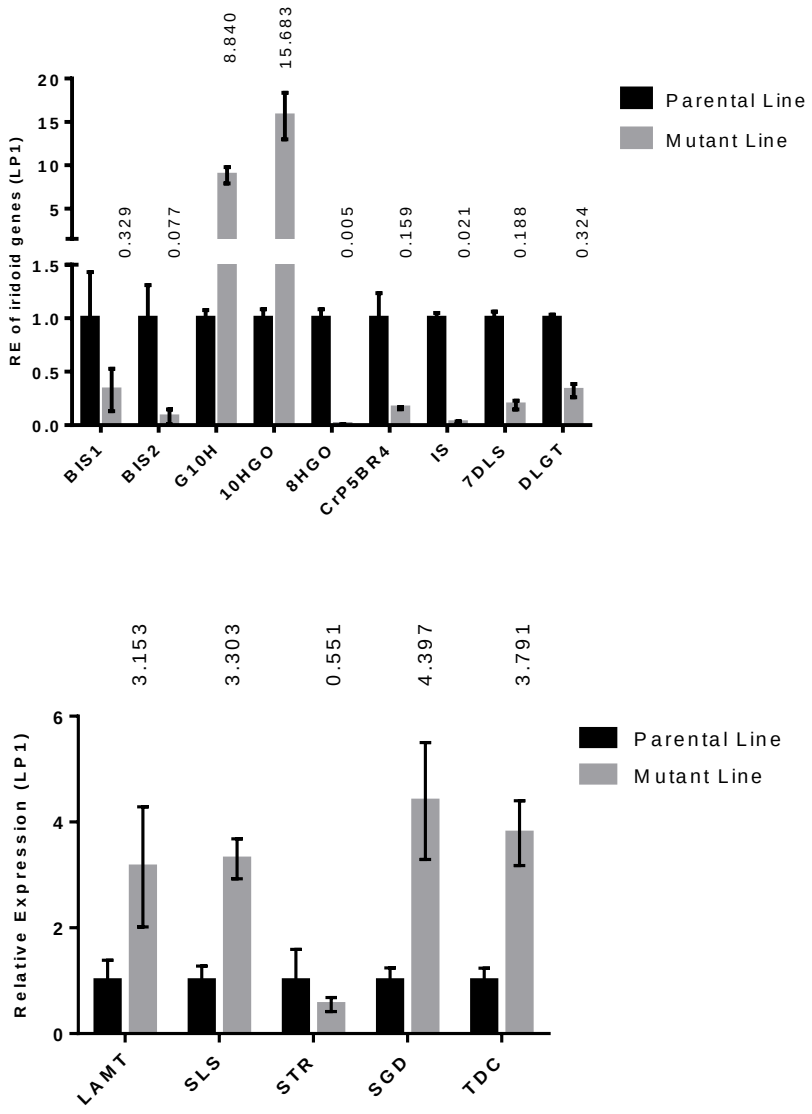

Figure 8: Comparison of iridoid and early stage MIA pathway gene expression profiles in leaf pair 1 of the mutant and WT plants. Error bars represent S.D. of four biological and four technical replicates. All datasets were normalized to WT expression profiles (1.000) Abbreviations: BIS1 and BIS2 (bHLH transcription factor 1 and 2); G10H (geraniol 10-hydroxylase); 10HGO (10-hydroxygeraniol oxidase), 8HGO (8-hydroxygeraniol oxidase), P5βR4 (progesterone 5β reductase-like 4), IS (Iridoid synthase), 7DLS (7-deoxyloganic acid synthase), DLGT (deoxyloganic acid glucosyltransferase), LAMT (loganic acid O-methyltransferase), SLS (secologanin synthase) SGD (strictosidine-β-glucosidase), TDC (tryptophan decarboxylase), STR (strictosidine synthase). The numbers above the bar refer to the fold- increase or decrease compared to WT expression profiles normalized to 1.000.

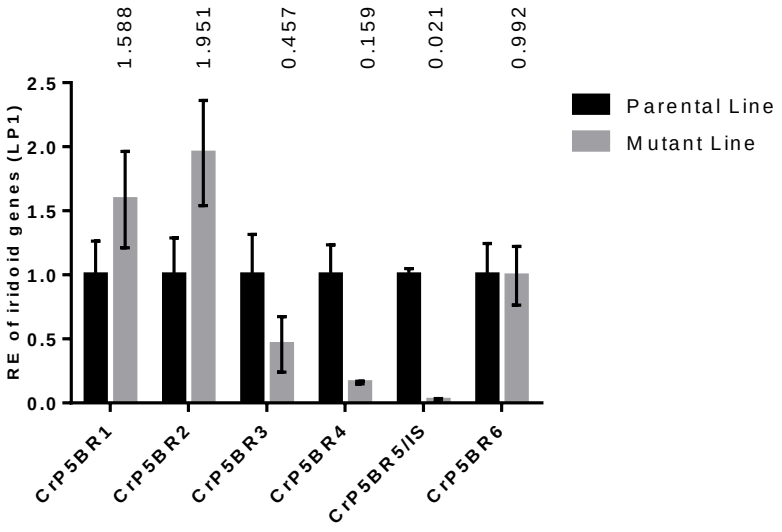

Figure 9: **Comparison of gene expression profiles in leaf pair 1 of six members of the progesterone 5B-reductase family from *C. roseus*.** Error bars represent S.D. of four biological and four technical replicates. All datasets were normalized to WT expression profiles (1.000). CrP5βR5 is the Iridoid Synthase (IS) previously identified in Geu-Flores et al., 2012. The numbers above the bar refer to the fold- increase or decrease compared to WT expression profiles normalized to 1.000.

3.4.2 Comparative expression profile of six progesterone 5β-reductase-like genes in the mutant background.

Previous studies (Munkert et al., 2015) showed that 6 progesterone 5β-reductase-like genes isolated from *C. roseus* (*CrP5βR1, CrP5βR2, CrP5βR3, CrP5βR4, CrP5βR4*5 and *CrP5βR6)* could functionally reduce 8-oxogeranial to iridoidial, raising the possibility that more than one of these genes might participate in iridoid biosynthesis in addition to the *C. roseus* iridoid synthase (*IS is CrP5βR*5*)* originally identified by Geu-Flores et al. (2012). Their studies concluded that *CrP5βR4* in addition to *CrP5βR5* might also be involved in iridoid biosynthesis. The results shown in Fig. 8 and in Fig. 9 describes expression of all 6 *CrP5βRs* and clearly suggests that loss of expression of *BIS1/BIS2* in the mutant (Fig. 8) strongly decreases *CrP5βR4* and *CrP5βR5* expression but not the other four progesterone 5β-reductase like genes (*CrP5βR1, CrP5βR2, CrP5βR3*, and *CrP5βR6*).

3.5 Grafting of line M2-1582 shoots to WT roots triggers MIA accumulation in mutant shoots

Nine individual mutant shoots containing a single leaf pair plus the stem were grafted separately onto the stem of the WT and grown *in vitro*. After one week of cultivation the four grafts that survived were used for further experimentation, with one leaf from each leaf pair harvested at 1-week post-graft and the 2nd leaf of the pair harvested three weeks post-graft, for extraction and iridoid/MIA analysis by UPLC-MS (Section 2.5 In Materials and methods). Catharanthine levels per gram fresh weight of leaf increased over 11- and 25-fold after 1 and 3 weeks respectively within the graft compared to the ungrafted mutant and reach over 51 % of those found in the ungrafted WT (Fig. 10). Vindoline levels per gram fresh weight of leaf increased over 27- and 46-fold after 1 and 3 weeks respectively within the graft compared to the

ungrafted mutant and reached over 67 % of the levels found in the ungrafted WT (Fig. 10). Catharanthine levels per leaf increased over 15- and 27-fold after 1 and 3 weeks respectively within the graft compared to the ungrafted mutant and reached over 27 % of the levels found in the ungrafted WT (Fig. 11). Vindoline levels per leaf increased over 7- and 16-fold after 1 and 3 weeks respectively within the graft compared to the ungrafted mutant and reached over 35 % of those found in the ungrafted WT (Fig. 11). Remarkably, secologanin levels per leaf also increase more than 6-fold over the first week and dropped by more than 60% by week three in leaves of the graft compared to those of un-grafted mutant. These results might be used to suggest that secologanin was being transported across the graft union into the mutant where it accumulated initially to be turned over to MIAs. As signs of senescence (browning and shriveling) began to appear in the grafted mutant after 3 weeks, it is conceivable that transport rates of secologanin might have been altered to account for the decline of secologanin in the 3-week time point.

The levels of 3´4´-anhydrovinblastine, 16-methoxytabersonine, deacetylvindoline, tabersonine, vindolidine and serpentine also rose considerably from zero within the grafted mutant compared to the ungrafted mutant line (Fig. 12). Together these results suggest that the secologanin transported across the graft union was being converted to all the major and minor MIAs normally found in the WT parent and that the pathways involved in MIA biosynthesis were as active in the mutant background as that of WT.

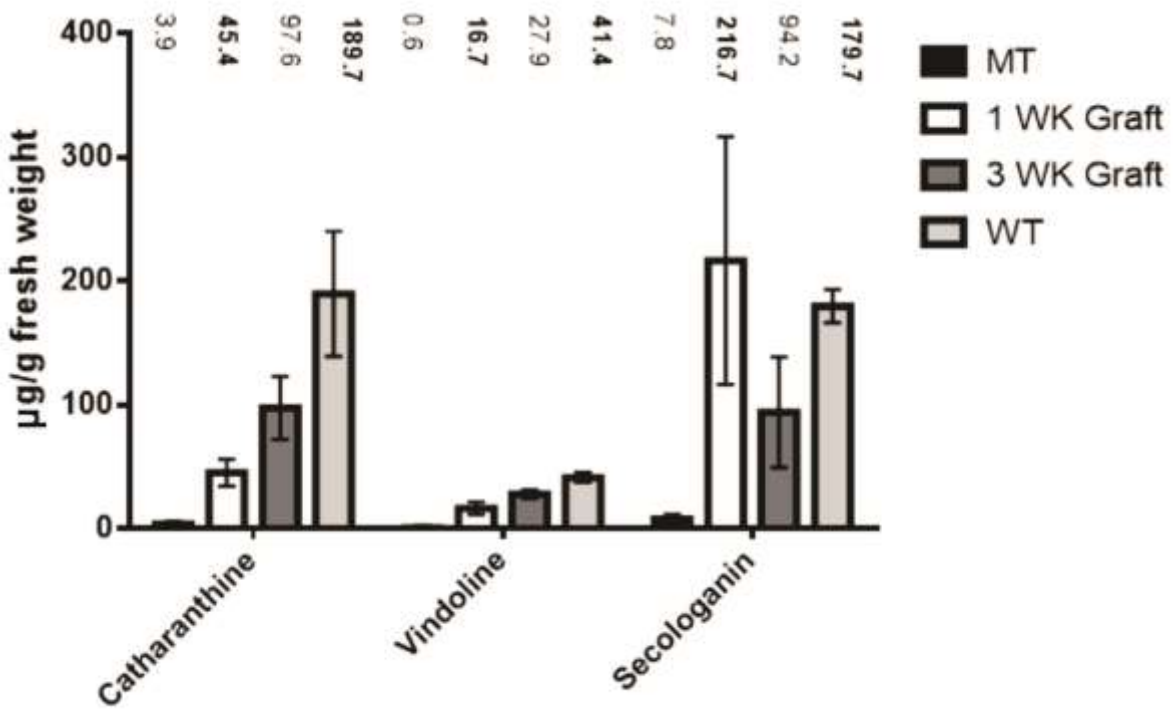

Figure 10: Comparison of leaf pair one samples for 1 week and 3 week grafts of mutant shoots grafted onto WT line shoots in vitro. µg/g fresh weight for four biological replicates each. The secologanin levels rise dramatically over the first week before beginning to fall, while the catharanthine and vindoline levels increase significantly approaching the WT line levels. The numbers above the bars refer to the µg of either catharanthine, vindoline or secologanin per gram fresh weight of LP1.

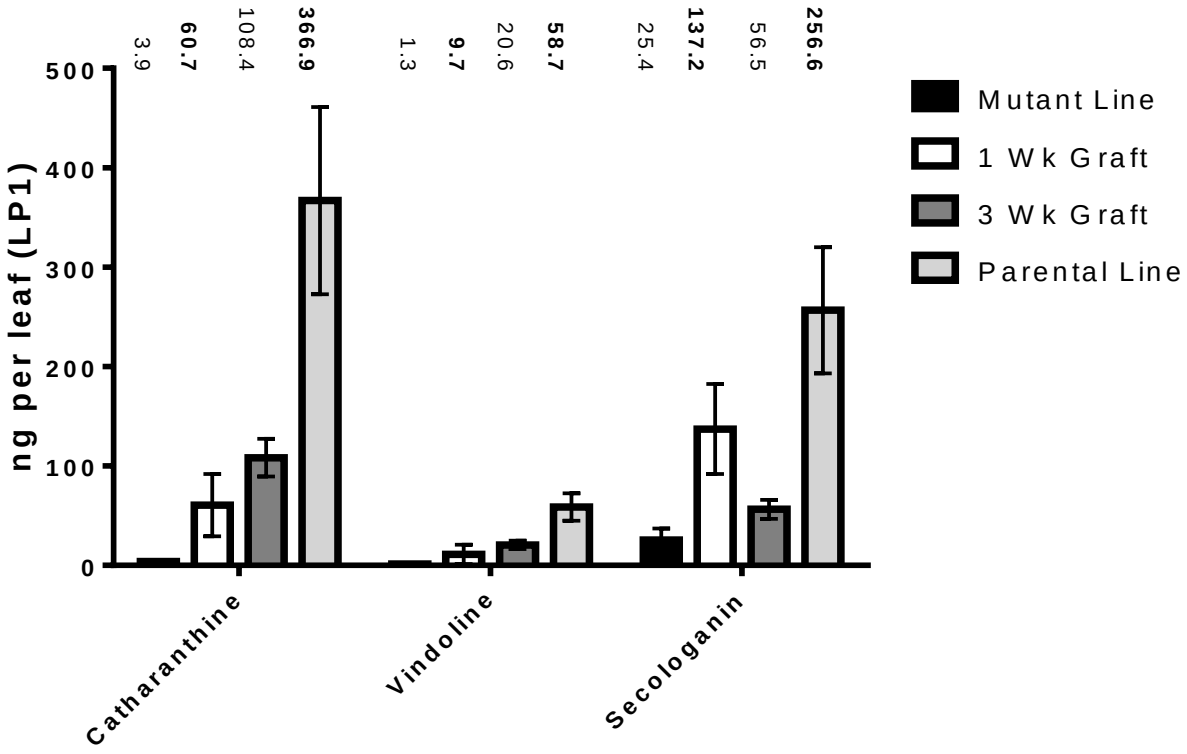

Figure 11: Catharanthine, vindoline, and secologanin accumulate in leaves of the M2-1582 line grafted on WT stems. The levels of catharanthine and vindoline increase progressively in leaves of the M2-1582 line after it was grafted onto WT stems, peaking in leaves of 3 week old grafts. Secologanin levels also rose considerably in the 1 week old graft but declined by the 3 week time point. The data represent catharanthine, vindoline and secologanin levels and standard deviations from 4 biological replicates.

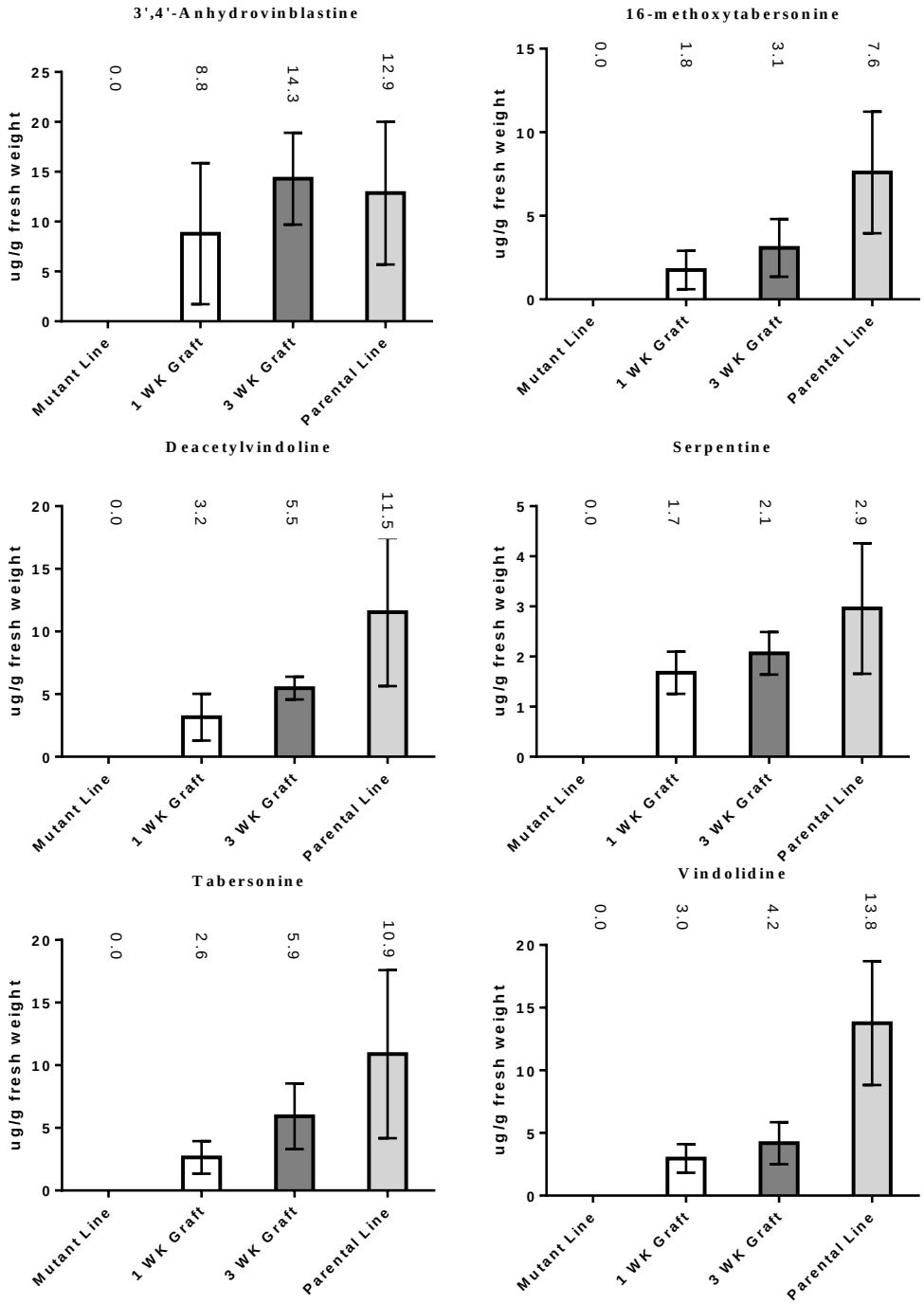

Figure 12: Minor MIAs accumulate in leaves of the M2-1582 line grafted on WT stems. The levels of 3′,4′-anhydroviblastine, 16-methoxytabersonine, deacetylvindoline, serpentine, tabersonine and vindolidine increase significantly in leaves of the M2-1582 line after it was grafted onto WT stems, approaching those found in the WT background in the **M2-1582** leaves of the 3 week-old graft. The data represent MIA levels and standard deviations from 4 biological replicates.

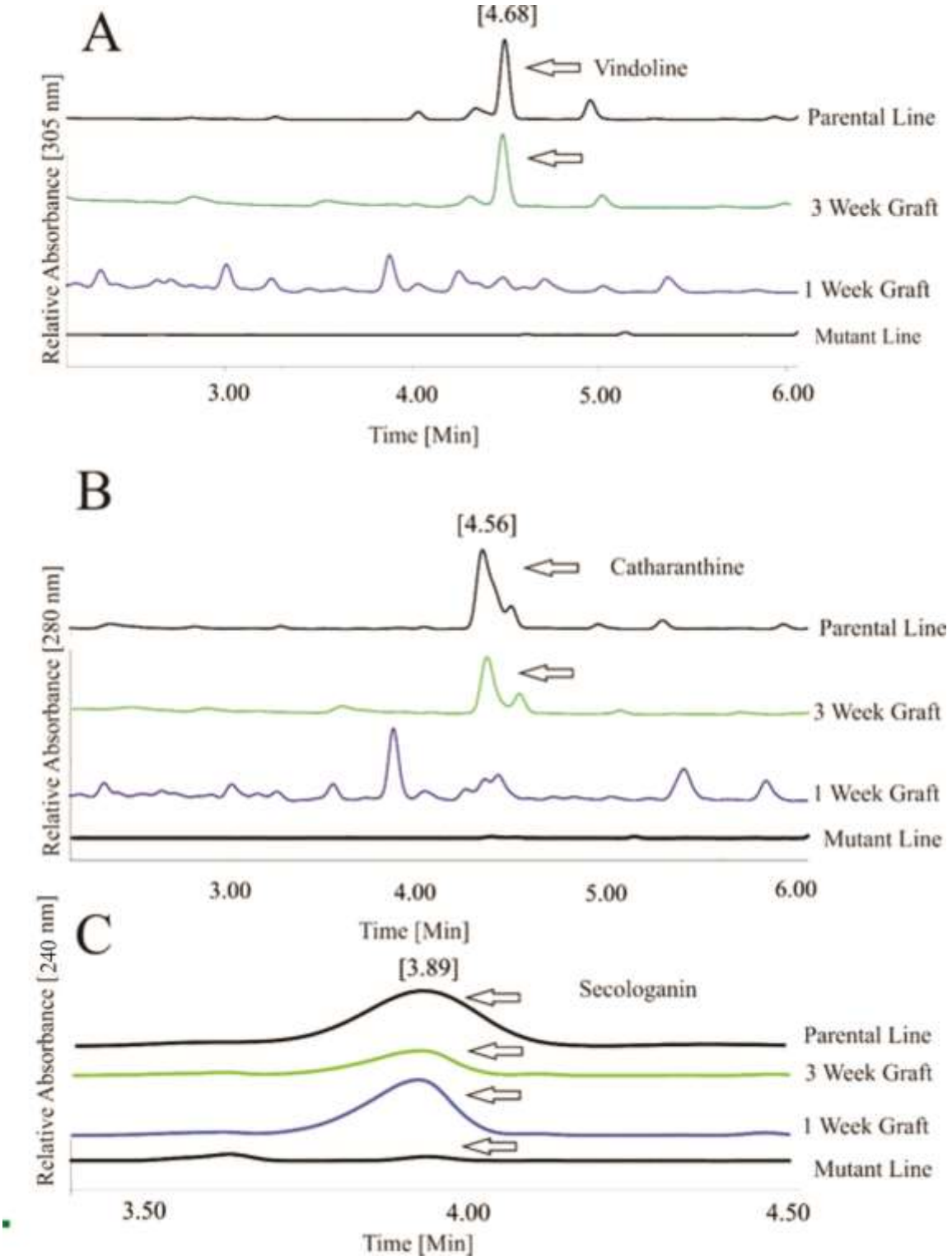

Figure 13: The grafts of line M2-1582 accumulate MIAs and secologanin. UPLC-MS profiles of MIAs were measured at A) 305 nm at B) 280 nm and at C) 240 nm to show elution of A) vindoline B) catharanthine and C) Secologanin in 1 and 3 week old mutant grafts compared to MT and WT control lines.

3.6 Secologanin feeding of whole mutant and wild-type line plants

The grafting experiments (Fig. 10-13) strongly suggested but did not prove that secologanin was being transported across the graft union into the mutant for eventual conversion to MIAs. This hypothesis was further tested by adding 1 mM secologanin to the culture media and allowing possible uptake of this iridoid through the roots of mutant or WT plants and by monitoring the accumulation of secologanin and production of MIAs in leaves over a 2-day period. The secologanin levels per gram fresh weight of leaf increase more than 6- and 12-fold in the M2-1582 line upon feeding of secologanin compared to the unfed control over the first and second day of feeding to reach over 38 % of the levels of secologanin found in the WT (Fig. 14). The catharanthine levels per gram fresh weight of leaf increase more than 3- and 4-fold in the M2-1582 line upon feeding of secologanin compared to the unfed control over the first and second day of feeding to reach over 23 % of the levels of catharanthine found in the WT (Fig. 14). The vindoline levels per gram fresh weight of leaf increased more than 5- and 8-fold fold in the M2-1582 line upon feeding of secologanin compared to the unfed control over the first and second day of feeding to reach over 24 % of the levels of vindoline found in the WT (Fig. 14). In contrast, the addition of secologanin to the WT did not enhance secologanin, catharanthine or vindoline levels over the 2-day period (Fig. 15). However, secologanin levels dropped by more than 24 and 58 % compared to the WT controls after the first and second day of secologanin feeding (Fig. 15). It should be noted that secologanin feeding of the mutant and WT plants showed important signs of toxicity in the leaves after 1 to 2 days (Fig. 16). The obvious and immediate increase in MIA levels from one and two-day feeding studies (Fig 14-15) support the results obtained in grafting experiment (Fig. 10-13) about the mobility of secologanin between organs within *C. roseus*. This data also strongly supports the molecular studies that suggest that

the trace MIA mutant is suppressed in the *BIS*- transcription factor-mediated induction and assembly of the iridoid component of the pathway (Fig 8-9).

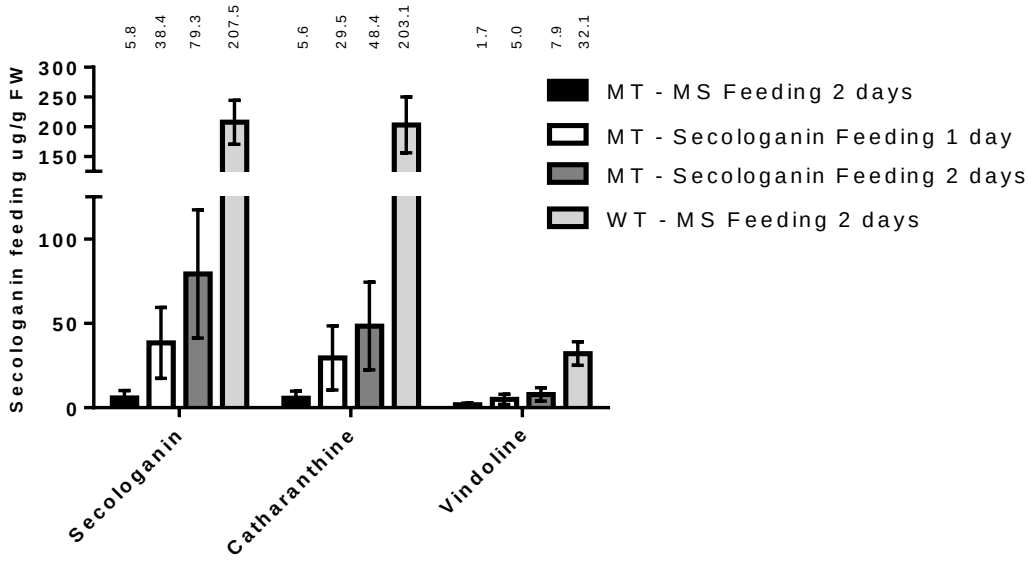

Figure 14: Feeding experiment using whole mutant plants in MS fluid with 1mM of secologanin added. MS fluid without secologanin was used as controls, both mutant (MT) and parental line (WT). Secologanin, catharanthine, and vindoline levels increased with secologanin feeding. The numbers above the bars refer to the µg of either catharanthine, vindoline or secologanin per gram fresh weight of LP1.

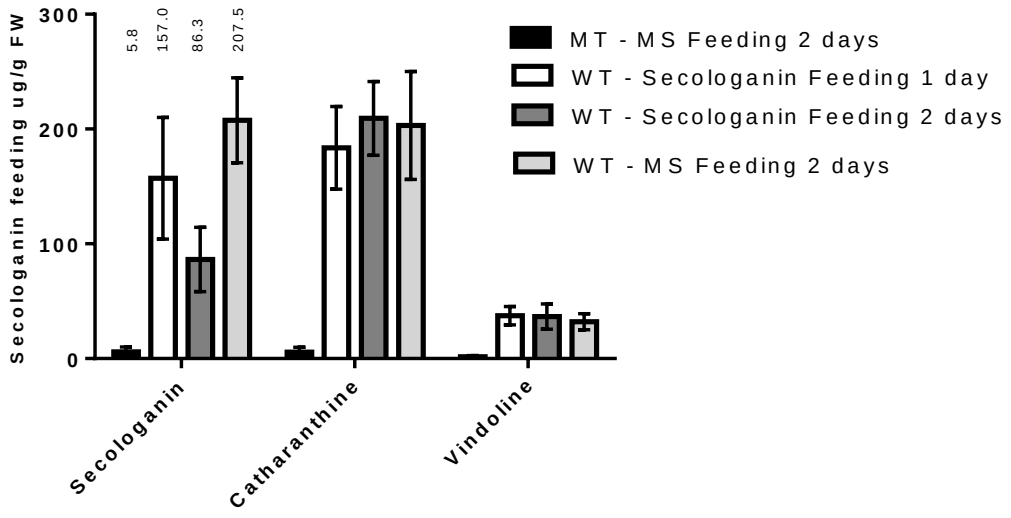

Figure 15: Secologanin feeding using whole wild-type line plants in MS fluid with 1mM of secologanin added. MS fluid without secologanin was used as controls, both mutant (MT) and parental line (WT). While the catharanthine and vindoline levels remained unchanged, the secologanin levels of the WT started to decrease rapidly once exposed to secologanin.

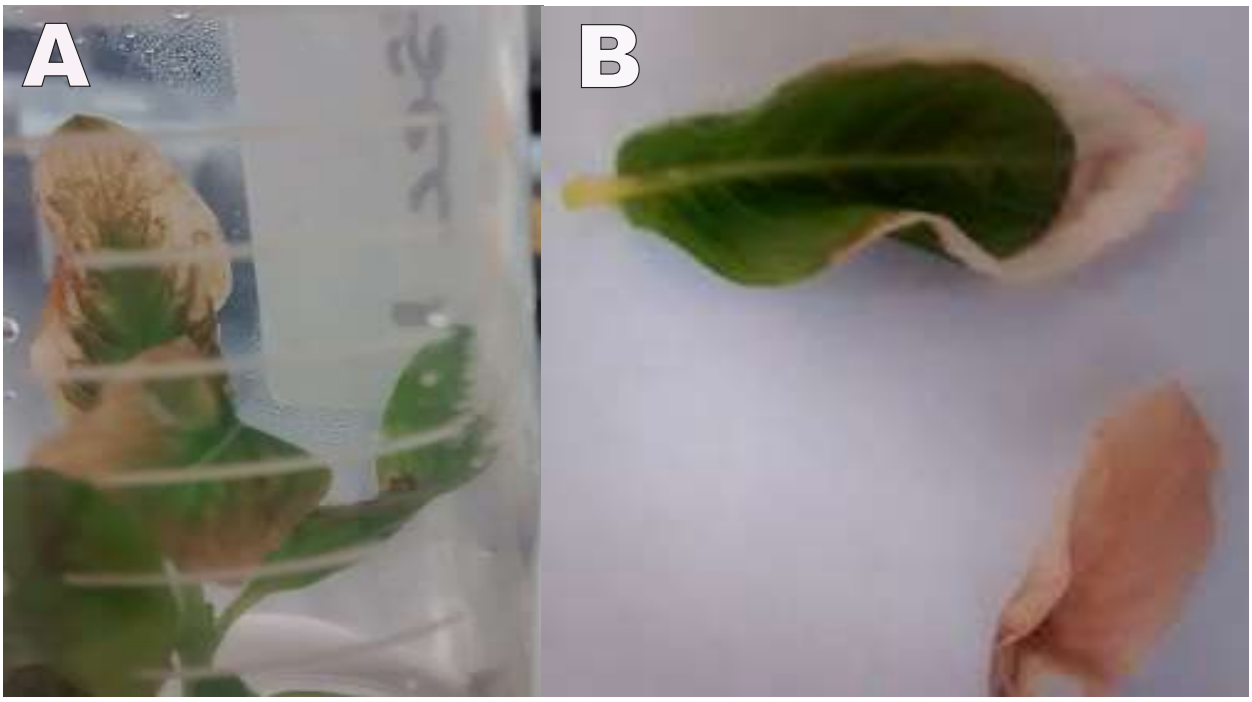

Figure 16: loss of colour and browning in leaves subjected to 1 mM of secologanin feeding. A shows the leaves of a WT line plant after 2 days of secologanin feeding. B shows two mutant leaves the top one after secologanin feeding of the roots for two days, and the bottom leaf is after secologanin feeding of the roots for six days.

4 Discussion

4.1 EMS mutagenesis combined with simple TLC screening identifies line M2-1582 that accumulates almost no MIAs and very little secologanin in *Catharanthus roseus*.

Despite its common use with crop plant varietal creation, EMS mutagenesis has been used sparingly in developing *C. roseus* lines that produce higher levels of MIAs or in producing mutants in MIA biosynthesis that could be used to understand biochemical pathways involved in their assembly (Kulkarni & Baskaran, 2015; Kulkarni et al., 1999). Recent studies in our laboratory have shown that a simple TLC screen for altered MIA profiles of leaf surface MIAs (Roepke et al., 2010) could be used by undergraduate students employed over a 16 week period over one summer to effectively screen between 3,000 to 4,000 *C. roseus* EMS mutants. This approach led undergraduate student, Mr. Michael Easson to identify three mutants with significantly altered MIA profiles including two separate low MIA lines, including the M2-1582 mutant out of 3000 mutants screened.

After identification of line M2-1582, it was cultivated in the greenhouse for approximately three months when it began to display diseases symptoms. Precautions were taken to create an in vitro line in case the diseases symptoms displayed by the mutant in the greenhouse became more serious. The greenhouse cultivated mutant did die a few weeks later, but the *in vitro* line survived and was micro-propagated to generate several hundred plants that could be used to investigate the phenotype of this line. Unfortunately, line M2-1582 grew slowly and displayed a number of unusual morphological characteristics including smaller leaves, shorter internodes and bundled short roots with altered fresh weights and a tendency to undergo premature senescence compared to the WT cultivated control (Fig.3-5; Table 2).

The low MIA phenotype of line M2-1582 is almost devoid of MIAs and low in secologanin, the iridoid precursor of all *C. roseus* MIAs

The quantitative analyses documented in the present thesis show that line M2-1582 accumulates 70- and 76-fold less catharanthine and vindoline in leaf pair one compared to the WT) (Fig 6), with minor MIAs not detected in the mutant (Fig 12). The mutant also accumulates 24-fold less secologanin compared to WT (Fig. 6) and together these results provided strong evidence that line M2-1582 did not accumulate MIAs because it was unable to produce secologanin. These results allowed our research efforts to focus on the identifying why the mutant no longer accumulated this precursor of MIA biosynthesis in the mutant.

4.2 The lack of BIS1/BIS2 expression in line M2-1582 accounts for suppression of the secologanin pathway.

Many transcription factors (TF) have been reported to modulate MIA gene expression including (ORCA2, ORCA3), G-box binding factors (GBFs), the MYB TF box P-binding factor-1 (BPF1), WRKY1, AT-hook TFs and EAR-domain containing TFs (Van Moerkercke et al., 2015, 2016). In addition, BIS1 and BIS2 have been shown to participate in the activation of geraniol synthase (GES), geraniol-10-hydroxylase (G10H), 8-hydroxygeraniol oxidoreductase (8HGO), iridoid synthase (IS), 7-deoxyloganetic acid glucosyltransferase (DLGT) and 7-deoxyloganic acid hydroxylase (7DLS) (Van Moerkercke et al., 2016). Both BIS1 and BIS2 transcription factors are preferentially expressed in IPAP cells upon induction by jasmonate treatment that leads to the enhanced accumulation of MIAs) (Van Moerkercke et al., 2016). The 3- and 13-fold decline in expression of *BIS1* and *BIS2* in line M2-1582 compared to the WT (Fig. 8 & 9) was accompanied with significant and variable reductions in transcription levels of

8HGO, *IS* (*CrP5βR5*), *CrP5βR4*, *7DLS* and *DLGT* (Fig. 8) These results showing a lack of expression of BIS and early iridoid pathway genes clearly explain why the mutant no longer produced the secologanin required for assembly of MIAs and the altered chemistry of the mutant.

In contrast transcript levels for LAMT, SLS, SGD, and TDC, expressed in the leaf epidermal cells, were each increased roughly 3 fold (Fig. 8), raising some new questions about the role(s) of BIS1 and BIS2, since they do not up-regulate gene MIA pathway gene expression in this cell type (Van Moerkercke et al. 2015, 2016). In contrast, the expression of *STR* was diminished almost 2-fold (Fig. 8) as suggested previously (Van Moerkercke et al., 2015, 2016). The meaning of these latter results (Fig. 8) remains to be established.

4.3 The conversion of 8-hydroxygeraniol to 8-oxogeranial involves the expression of 8-HGO rather than 10-HGO.

It has been suggested that the biosynthesis of 8-oxogeranial might involve the participation of an NADP+-dependent alcohol dehydrogenase (10HG) (Krithika et al., 2015; Miettinen et al., 2014) and/or an NAD+ dependent oxidoreductase (8HGO) (Krithika et al., 2015; Miettinen et al., 2014). While both gene products catalyze this reaction, *in-situ* hybridization studies localized 8-HGO expression to IPAP cells, while 10-HGO has not. (Miettinen et al., 2014) Present studies showed that expression of *G10H* and *10HGO* was increased 8- and 15-fold, respectively, in line M2-1582 compared to the WT, while expression of *8HGO* declined almost 200-fold in the mutant (Fig. 8). These results together with the localization of gene expression to IPAP cells (Miettinen et al., 2014) supports *8HGO* as the legitimate gene involved in the secologanin biosynthesis rather than *10HGO*.

4.4 Both *CrP5βR4 and CrP5βR5 play a role in iridoid biosynthesis*

Munkert et al., (2015) found that iridoid synthase is part of a family of six *Catharanthus roseus P5βR5 genes. In addition to* CrP5βR5/IS (Geu-Flores et al., 2012), *three others* CrP5βR1, CrP5βR2, and CrP5βR4, able to reduce 8-oxogeranial (Munkert et al., 2015). *While all six* CrP5βRs are localized to the cytosol, only CrP5βR4 and CrP5βR5/IS were expressed at high absolute transcript levels and localized to the IPAP cells (Munkert et al., 2015). Our findings (Fig. 8 and Fig. 9) support that CrP5βR4 may play a role as a redundancy to CrP5βR5/IS in iridoid biosynthesis.

4.5 Translocation of pre-MIAs from the roots to the shoots

The intercellular and intra-cellular transportation of MIAs and pre-MIAs in *Catharanthus roseus* is well understood (Facchini & De Luca, 2008; Shitan et al., 2014a). However, inter-organ transportation of pre-MIAs or MIAs had not been confirmed.

Evidence for long-distance transportation or translocation of alkaloids in other species of plants have been demonstrated via both the phloem (quinolizidine, pyrrolizidine, and indolizidine) and xylem (nicotine and berberine) (Shitan et al., 2014a) and evidence of long-distance translocation within the phloem of iridoid glucosides has been found in antirrhinoside and catalpol has also been demonstrated (Beninger et al., 2008, 2009). However, this is the first demonstration of long-distance translocation of pre-MIAs in *Catharanthus roseus* with evidence of secologanin or other pre-MIA translocation for the roots of a wild type stock to the leaves of non-alkaloid producing mutant line shoots.

4.6 Future Work

Significant future work can be derived with this mutant line. RNA sequencing and comparative bioinformatics of mutant and parental lines may direct future work through indicating the source of the mutation, up or down regulated genes and transcription factors as well as the search for novel transporters.

Sequencing and bioinformatics have been used to elucidate missing steps in the biosynthesis of specialized plant metabolites (De Luca et al., 2012; Liscombe et al., 2010).

As EMS mutagenesis results in point mutations, a mutant in a transcription factor may not result in changes in gene expression levels, while a mutation in a promoter region is more likely to. Using a sequencing method such as RNAseq would provide confirmation for iridoid expression levels and indicate promoter region sequences to be cloned and sequenced to identify potential mutations (Thamm, 2014).

The phenotypical characteristics of the mutant line give rise to experiments. The mutant line grows slowly, does not flower and experiences premature senescence, and the mutation may have an impact on flower signaling as well as signaling for senescence. The literature does suggest some genes that influence these characteristics, but the mutation in M2-1582 will likely lead to a promoter region that is currently not known to affect senescence, flowering, and growth rate. Golldack et al. (2002) demonstrated that an *Arabidopsis thaliana* line with a mutation in the matrix metalloproteinase At2-MMP gene showed slow growth of roots, shoots, and leaves, late flowering, rapid degradation of chlorophyll in the leaves and premature senescence. Vogelmann et al. (2012) demonstrated that *Arabidopsis thaliana* with mutant senescence-

associated ubiquitin ligase1 (saul1) genes accumulated the transcription factor ORESARA1 and experienced early senescence.

Experimentation with hormone levels in the media may affect the lack of primary root growth in the mutant, despite significant overall root growth as well as early senescence and lack of flowering. The hormone ethylene is an essential plant growth regulator and Yang et al. (2008) found that an *Arabidopsis thaliana* line with mutant ethylene receptor ETR1-1 showed early senescence prior to flowering. Jasmonic acid also plays a significant role in growth and senescence, with research indicating that there may be significant interactions between the hormones ethylene and jasmonic acid in determining the growth and senescence of plants (Kim, Chang, & Tucker, 2015).

5 Conclusion

The present work showed the value of EMS mutagenesis in creating *Catharanthus roseus* mutants with novel phenotypes. The iridoid and MIA profile of EMS mutant M2-1582 was successfully characterized finding all measured alkaloids to be extremely low if present at all and parts of the iridoid pathway, specifically 8HGO, CrP5βR4 and CrP5βR5/IS, to be severely compromised. The results of this study support previous research suggesting a role for BIS1 and BIS2 in activating early iridoid pathway genes in the IPAP cells as well as research suggesting that CrP5βR4 plays a redundant role with CrP5βR5/IS in iridoid biosynthesis.

Finally, this work used both feeding experiments with secologanin as well as the grafting of low alkaloid mutant (M2-0754) shoots onto WT roots to demonstrate the appearance of alkaloids in the low alkaloid mutant leaves demonstrating long-distance translocation of pre-MIAs in *Catharanthus roseus*.

6. References

Ahloowalia, B. S., Maluszynski, M., & Nichterlein, K. (2004). Global impact of mutation-derived varieties. *Euphytica*, *135*(2), 187–204.

Asada, K., Salim, V., Masada-Atsumi, S., Edmunds, E., Nagatoshi, M., & De Luca, V. (2013). A 7-deoxyloganetic acid glucosyltransferase contributes a key step in secologanin biosynthesis in Madagascar periwinkle. *The Plant Cell*, *25*(10), 4123–34.

Baldwin, I. T., Schmelz, E. a., & Ohnmeiss, T. E. (1994). Wound-induced changes in root and shoot jasmonic acid pools correlate with induced nicotine synthesis in Nicotiana sylvestris spegazzini and comes. *Journal of Chemical Ecology*, *20*(8), 2139–2157.

Baldwin, I. T., Sims, C. L., & Kean, S. E. (1990). The reproductive consequences associated with inducible alkaloidal responses in wild tobacco. *Ecology*.

Baldwin, I. T., Zhang, Z. P., Diab, N., Ohnmeiss, T. E., McCloud, E. S., Lynds, G. Y., & Schmelz, E. A. (1997). Quantification, correlations and manipulations of wound-induced changes in jasmonic acid and nicotine in Nicotiana sylvestris. *Planta*, *201*(4), 397–404.

Beninger, C. W., Cloutier, R. R., & Grodzinski, B. (2008). The iridoid glucoside, antirrhinoside, from Antirrhinum majus L. has differential effects on two generalist insect herbivores. *Journal of Chemical Ecology*, *34*(5), 591–600.

Beninger, C. W., Cloutier, R. R., & Grodzinski, B. (2009). A comparison of antirrhinoside distribution in the organs of two related Plantaginaceae species with different reproductive strategies. *Journal of Chemical Ecology*, *35*(11), 1363–1372.

Beninger, C. W., Cloutier, R. R., Monteiro, M. A., & Grodzinski, B. (2007). The distribution of two major iridoids in different organs of Antirrhinum majus L. at selected stages of development. *Journal of Chemical Ecology*, *33*(4), 731–747.

Bowsher, C., Steer, M., & Tobin, A. (2008). *Plant Biochemistry* (1st editio). Garland Science; Taylor & Francis Group.

Braun, D. M., Wang, L., & Ruan, Y. L. (2014). Understanding and manipulating sucrose phloem loading, unloading, metabolism, and signalling to enhance crop yield and food security. *Journal of Experimental Botany*.

Buchanan, B. B., Gruissem, W., & Jones, R. L. (2015). *Biochemistry & Molecular Biology of Plants*. *Journal of Chemical Information and Modeling* (2nd ed., Vol. 53). John Wiley & Sons, Ltd.

Burlat, V., Oudin, A., Courtois, M., Rideau, M., & St-Pierre, B. (2004). Co-expression of three MEP pathway genes and geraniol 10-hydroxylase in internal phloem parenchyma of *Catharanthus roseus* implicates multicellular translocation of intermediates during the biosynthesis of monoterpene indole alkaloids and isoprenoid-derive. *Plant Journal*, *38*(1), 131–141.

Chahed, K., Oudin, A., Guivarc'h, N., Hamdi, S., Chenieux, J. C., Rideau, M., & Clastre, M. (2000). 1-Deoxy-D-xylulose 5-phosphate synthase from periwinkle: cDNA identification and induced gene expression in terpenoid indole alkaloid-producing cells. *Plant Physiology and Biochemistry*, *38*(7–8), 559–566.

Chen, L. Q., Qu, X. Q., Hou, B. H., Sosso, D., Osorio, S., Fernie, A. R., & Frommer, W. B. (2012). Sucrose Efflux Mediated by SWEET Proteins as a Key Step for Phloem Transport.

Science, *335*(6065), 207–211.

Chen, S., Petersen, B. L., Olsen, C. E., Schulz, A., & Halkier, B. A. (2001). Long-distance phloem transport of glucosinolates in Arabidopsis. *Plant Physiology*, *127*, 194–201.

Collu, G., Garcia, A. A., Van der Heijden, R., & Verpoorte, R. (2002). Activity of the cytochrome P450 enzyme geraniol 10-hydroxylase and alkaloid production in plant cell cultures. *Plant Science*, *162*(1), 165–172.

Collu, G., Unver, N., Peltenburg-Looman, A. M., Van der Heijden, R., Verpoorte, R., & Memelink, J. (2001). Geraniol 10-hydroxylase, a cytochrome P450 enzyme involved in terpenoid indole alkaloid biosynthesis. *FEBS Letters*, *508*(2), 215–20.

Contin, A., Van Der Heijden, R., Lefeber, A. W. M., & Verpoorte, R. (1998). The iridoid glucoside secologanin is derived from the novel triose phosphate/pyruvate pathway in a *Catharanthus roseus* cell culture. *FEBS Letters*, *434*(3), 413–416.

Dawson, R. . (1941). Localization of the nicotine synthetic mechanism in the tobacco plant. *Science*, *94*, 396–397.

De Carolis, E., Chan, F., Balsevich, J., & De Luca, V. (1990). Isolation and Characterization of a 2-Oxoglutarate Dependent Dioxygenase Involved in the Second-to-Last Step in Vindoline Biosynthesis. *Plant Physiology*, *94*(3), 1323–9.

De Carolis, E., & De Luca, V. (1993). Purification, characterization, and kinetic analysis of a 2-oxoglutarate- dependent dioxygenase involved in vindoline biosynthesis from *Catharanthus roseus*. *Journal of Biological Chemistry*, *268*(8), 5504–5511.

De Carolis, E., & De Luca, V. (1994). 2-Oxoglutarate-dependent dioxygenase and related

enzymes: Biochemical characterization. *Phytochemistry*.

De Luca, V., Balsevich, J., Tyler, R. ., & Kurz, W. (1987). Characterization of a novel N-methyltransferase (NMT) from *Catharanthus roseus* plants. *Plant Cell Reports*, *6*, 458–461.

De Luca, V., Marineau, C., & Brisson, N. (1989). Molecular cloning and analysis of cDNA encoding a plant tryptophan decarboxylase: comparison with animal dopa decarboxylases. *Proceedings of the National Academy of Sciences of the United States of America*, *86*(8), 2582–2586.

De Luca, V., Salim, V., Levac, D., Masada-Atsumi, S., & Yu, F. (2012). *Chapter Ten - Discovery and Functional Analysis of Monoterpenoid Indole Alkaloid Pathways in Plants In: Methods in Enzymology Ed. by David A. Hopwood*.

El-Sayed, M., & Verpoorte, R. (2007). Catharanthus terpenoid indole alkaloids: Biosynthesis and regulation. *Phytochemistry Reviews*.

Facchini, P. J., & De Luca, V. (2008). Opium poppy and Madagascar periwinkle: Model non-model systems to investigate alkaloid biosynthesis in plants. *Plant Journal*, *54*(4), 763–784.

FAO/IAEA. (2016). FAO/IAEA Mutant variety database. Retreived August 16, 2016 from https://mvd.iaea.org/.

Geerlings, A., Ibañez, M. M., Memelink, J., Van Der Heijden, R., & Verpoorte, R. (2000). Molecular cloning and analysis of strictosidine beta-D-glucosidase, an enzyme in terpenoid indole alkaloid biosynthesis in *Catharanthus roseus*. *The Journal of Biological Chemistry*, *275*(5), 3051–3056.

Gerasimenko, I., Sheludko, Y., Ma, X., & Stöckigt, J. (2002). Heterologous expression of a

Rauvolfia cDNA encoding strictosidine glucosidase, a biosynthetic key to over 2000 monoterpenoid indole alkaloids. *European Journal of Biochemistry*, *269*(8), 2204–2213.

Geu-Flores, F., Sherden, N. H., Courdavault, V., Burlat, V., Glenn, W. S., Wu, C., & O'Connor, S. E. (2012). An alternative route to cyclic terpenes by reductive cyclization in iridoid biosynthesis. *Nature*, *492*(7427), 138–142.

Golldack, D., Popova, O. V., & Dietz, K. J. (2002). Mutation of the matrix metalloproteinase At2-MMP inhibits growth and causes late flowering and early senescence in Arabidopsis. *Journal of Biological Chemistry*, *277*(7), 5541–5547.

Guirimand, G., Courdavault, V., Lanoue, A., Mahroug, S., Guihur, A., St-Pierre, B., & Burlat, V. (2010). Strictosidine activation in Apocynaceae: towards a "nuclear time bomb"? *BMC Plant Biology*, *10*, 182.

Guirimand, G., Guihur, A., Ginis, O., Poutrain, P., Oudin, A., St-Pierre, B., & Courdavault, V. (2011). The subcellular organization of strictosidine biosynthesis in *Catharanthus roseus* epidermis highlights several trans-tonoplast translocations of intermediate metabolites. *FEBS Journal*, *278*(5), 749–763.

Hildreth, S. B., Gehman, E. A., Yang, H., Lu, R. H., Harich, K. C., Yu, S., & Jelesko, J. G. (2011). Tobacco nicotine uptake permease (NUP1) affects alkaloid metabolism. *Proceedings of the National Academy of Sciences*, *108*(44), 18179–18184.

Howe, G. A., & Jander, G. (2008). Plant immunity to insect herbivores. *Annual Review of Plant Biology*, *59*, 41–66.

Irmler, S., Schröder, G., St-Pierre, B., Crouch, N. P., Hotze, M., Schmidt, J., & Schröder, J.

(2000). Indole alkaloid biosynthesis in *Catharanthus roseus*: New enzyme activities and identification of cytochrome P450 CYP72A1 as secologanin synthase. *Plant Journal*, *24*(6), 797–804.

Kehr, J. (2009). Long-distance transport of macromolecules through the phloem. *Biology Reports*, *13410*, 31–1.

Kim, J., Chang, C., & Tucker, M. L. (2015). To grow old: regulatory role of ethylene and jasmonic acid in senescence. *Frontiers in Plant Science*, *6*(January), 20.

Krithika, R., Srivastava, P. L., Rani, B., Kolet, S. P., Chopade, M., Soniya, M., & Thulasiram, H. V. (2015). Characterization of 10-hydroxygeraniol dehydrogenase from *Catharanthus roseus* reveals cascaded enzymatic activity in iridoid biosynthesis. *Scientific Reports*, *5*, 8258.

Kulkarni, R. N., & Baskaran, K. (2015). Increasing total leaf alkaloid concentrations in periwinkle (*Catharanthus roseus*) by combining the macro-mutant traits of two induced leaf. *The Journal of Horticultural Science and Biotechnology*, *316*(August 2016), 513–518.

Kulkarni, R. N., Baskaran, K., Chandrashekara, R. S., & Kumar, S. (1999). Inheritance of morphological traits of periwinkle mutants with modified contents and yields of leaf and root alkaloids. *Plant Breeding*, *118*(1), 71–74.

Kutchan, T. M. (1989). Expression of enzymatically active cloned strictosidine synthase from the higher plant Rauvolfia serpentina in Escherichia coli. *FEBS Letters*, *257*(1), 127–130.

Lange, B. M., & Croteau, R. (1999). Isopentenyl diphosphate biosynthesis via a mevalonate-independent pathway: isopentenyl monophosphate kinase catalyzes the terminal enzymatic

step. *Proceedings of the National Academy of Sciences of the United States of America*, *96*(24), 13714–9.

Li, L., He, Z., Pandey, G. K., Tsuchiya, T., & Luan, S. (2002). Functional cloning and characterization of a plant efflux carrier for multidrug and heavy metal detoxification. *Journal of Biological Chemistry*, *277*, 5360–5368.

Lichtenthaler, H. K. (1999). The 1-Deoxy-D-Xylulose-5-Phosphate Pathway of Isoprenoid Biosynthesis in Plants. *Annual Review of Plant Physiology and Plant Molecular Biology*, *50*(1), 47–65.

Liscombe, D. K., Usera, A. R., & O'Connor, S. E. (2010). Homolog of tocopherol C methyltransferases catalyzes N methylation in anticancer alkaloid biosynthesis. *Proceedings of the National Academy of Sciences of the United States of America*, *107*(44), 18793–18798.

Luijendijk, T. J. C., Stevens, L. H., & Verpoorte, R. (1998). Purification and characterisation of strictosidine beta-D-glucosidase from *Catharanthus roseus* cell suspension cultures. *Plant Physiology and Biochemistry*, *36*(6), 419–425.

Mangaiyarkarasi, R., Girija, M., Gnanamurthy, S., & Don, C. L. G. (2014). Mutagenic effectiveness and efficiency of gamma rays and ethyl methane sulphonate in *Catharanthus roseus*. *Int. J. Curr. Microbiology*, *3*(5), 881–889.

McCallum, C. M., Comai, L., Greene, E. A., & Henikoff, S. (2000). Targeted screening for induced mutations. *Nature Biotechnology*, *18*(4), 455–457.

Meehan, T. D., & Coscia, C. J. (1973). Hydroxylation of geraniol and nerol by a monooxygenase

from Vinca rosea. *Biochemical and Biophysical Research Communications*, *53*(4), 1043–1048.

Miettinen, K., Dong, L., Navrot, N., Schneider, T., Burlat, V., Pollier, J., … Werck-Reichhart, D. (2014). The seco-iridoid pathway from *Catharanthus roseus*. *Nature Communications*, *5*, 3606.

Mithöfer, A., & Boland, W. (2012). Plant defense against herbivores: Chemical aspects. *Annual Review of Plant Biology*, *63*, 431–450.

Morita, M., Shitan, N., Sawada, K., Van Montagu, M. C. E., Inzé, D., Rischer, H., … Yazaki, K. (2009). Vacuolar transport of nicotine is mediated by a multidrug and toxic compound extrusion (MATE) transporter in Nicotiana tabacum. *Proceedings of the National Academy of Sciences of the United States of America*, *106*(7), 2447–2452.

Morita, Y., Kodama, K., Shiota, S., Mine, T., Kataoka, A., Mizushima, T., & Tsuchiya, T. (1998). NorM, putative multidrug efflux protein, of Vibrio parahaemolyticus and its homolog in Escherichia coli. *Antimicrobial Agents and Chemotherapy*, *42*(7), 1778–1782.

Mudge, K. W. (2015). Top Wedge Grafting - Hort 400 Plant Propagation Web site autotutorial. Retrieved September 1, 2015, from https://courses.cit.cornell.edu/hort494/mg/methods.alpha/TWGMeth.html

Munkert, J., Pollier, J., Miettinen, K., Van Moerkercke, A., Payne, R., Müller-Uri, F., … Goossens, A. (2015). Iridoid synthase activity is common among the plant progesterone 5β-reductase family. *Molecular Plant*, *8*(1), 136–152.

Murata, J., Roepke, J., Gordon, H., & De Luca, V. (2008). The leaf epidermome of *Catharanthus*

roseus reveals its biochemical specialization. *The Plant Cell*, *20*(3), 524–542.

Nagatoshi, M., Terasaka, K., Nagatsu, A., & Mizukami, H. (2011). Iridoid-specific glucosyltransferase from Gardenia jasminoides. *Journal of Biological Chemistry*, *286*(37), 32866–32874. https://doi.org/10.1074/jbc.M111.242586

O'Connor, S. E., & Maresh, J. J. (2006). Chemistry and biology of monoterpene indole alkaloid biosynthesis. *Nat. Prod. Rep.*, *23*, 532–47.

Omote, H., Hiasa, M., Matsumoto, T., Otsuka, M., & Moriyama, Y. (2006). The MATE proteins as fundamental transporters of metabolic and xenobiotic organic cations. *Trends in Pharmacological Science*, *27*, 587–593.

Papon, N., Bremer, J., Vansiri, A., Andreu, F., Rideau, M., & Crèche, J. (2005). Cytokinin and ethylene control indole alkaloid production at the level of the MEP/terpenoid pathway in *Catharanthus roseus* suspension cells. *Planta Medica*, *71*(6), 572–574.

Phillips, M. A., Leon, P., Boronat, A., & Rodriguez-Concepcion, M. (2008). The plastidial MEP pathway: unified nomenclature and resources. *Trends in Plant Science*, *13*(12), 619–623.

Qu, Y., Easson, M. L. a. E., Froese, J., Simionescu, R., Hudlicky, T., & De Luca, V. (2015). Completion of the seven-step pathway from tabersonine to the anticancer drug precursor vindoline and its assembly in yeast. *Proceedings of the National Academy of Sciences*, *112*(19), 201501821.

Rani, N., & Kumar, K. (2015). EMS induced mitotic abnormalities in *Catharanthus roseus* (L.) G. Don. *Journal of Global Biosciences*, *4*(1), 1816–1823.

Rodríguez-Concepción, M., & Boronat, A. (2002). Elucidation of the methylerythritol phosphate

pathway for isoprenoid biosynthesis in bacteria and plastids. A metabolic milestone achieved through genomics. *Plant Physiology*, *130*(3), 1079–1089.

Roepke, J., Salim, V., Wu, M., Thamm, A. M., Murata, J., Ploss, K., … De Luca, V. (2010). Vinca drug components accumulate exclusively in leaf exudates of Madagascar periwinkle. *Proc Natl Acad Sci U S A*, *107*(34), 15287–15292.

Salim, V. (2013). *Functional characterization of monoterpenoid indole alkaloid (MIA) biosynthetic genes in Catharanthus roseus*. Brock University.

Salim, V., Wiens, B., Masada-Atsumi, S., Yu, F., & De Luca, V. (2014). 7-Deoxyloganetic acid synthase catalyzes a key 3 step oxidation to form 7-deoxyloganetic acid in *Catharanthus roseus* iridoid biosynthesis. *Phytochemistry*, *101*, 23–31.

Shitan, N., Hayashida, M., & Yazaki, K. (2015). Translocation and accumulation of nicotine via distinct spatio-temporal regulation of nicotine transporters in Nicotiana tabacum. *Plant Signaling and Behavior*, *10*(7), e1035852–e1035855.

Shitan, N., Kato, K., & Shoji, T. (2014). Alkaloid transporters in plants. *Plant Biotechnology*, *31*(5), 453–463.

Shitan, N., Minami, S., Morita, M., Hayashida, M., Ito, S., Takanashi, K., … Yazaki, K. (2014). Involvement of the leaf-specific multidrug and toxic compound extrusion (mate) transporter Nt-JAT2 in vacuolar sequestration of nicotine in nicotiana tabacum. *PLoS ONE*, *9*(9).

Shoji, T., Inai, K., Yazaki, Y., Sato, Y., Takase, H., Shitan, N., … Hashimoto, T. (2009). Multidrug and toxic compound extrusion-type transporters implicated in vacuolar sequestration of nicotine in tobacco roots. *Plant Physiology*, *149*(2), 708–718.

Shu, Q.Y., Forster, B.P., Nakagawa, H. (2012). *Plant Mutation Breeding and Biotechnology*. *Journal of Chemical Information and Modeling* (Vol. 53). CABI.

Sikora, P., Chawade, A., Larsson, M., Olsson, J., & Olsson, O. (2011). Mutagenesis as a tool in plant genetics, functional genomics, and breeding. *International Journal of Plant Genomics*, *2011*, 1–13.

Simkin, A. J., Miettinen, K., Claudel, P., Burlat, V., Guirimand, G., Courdavault, V., … Clastre, M. (2013). Characterization of the plastidial geraniol synthase from Madagascar periwinkle which initiates the monoterpenoid branch of the alkaloid pathway in internal phloem associated parenchyma. *Phytochemistry*, *85*, 36–43.

St-Pierre, B., & De Luca, V. (1995). A Cytochrome P-450 Monooxygenase Catalyzes the First Step in the Conversion of Tabersonine to Vindoline in *Catharanthus roseus*. *Plant Physiology*, *109*(1), 131–139.

St-Pierre, B., Laflamme, P., Alarco, A. M., & De Luca, V. (1998). The terminal O-acetyltransferase involved in vindoline biosynthesis defines a new class of proteins responsible for coenzyme A-dependent acyl transfer. *Plant Journal*, *14*(6), 703–713.

Suttipanta, N., Pattanaik, S., Gunjan, S., Xie, C. H., Littleton, J., & Yuan, L. (2007). Promoter analysis of the *Catharanthus roseus* geraniol 10-hydroxylase gene involved in terpenoid indole alkaloid biosynthesis. *Biochimica et Biophysica Acta - Gene Structure and Expression*, *1769*(2), 139–148.

Thamm, A. M. (2014). *Catharanthus roseus mutant altered in monoterpenoid indole alkaloid biosynthesis*.

Van Der Heijden, R., Jacobs, D. I., Snoeijer, W., Hallard, D., & Verpoorte, R. (2004). The Catharanthus alkaloids: pharmacognosy and biotechnology. *Current Medicinal Chemistry*, *11*(5), 607–628.

Van Moerkercke, A., Steensma, P., Gariboldi, I., Espoz, J., Purnama, P. C., Schweizer, F., … Goossens, A. (2016). The basic helix-loop-helix transcription factor BIS2 is essential for monoterpenoid indole alkaloid production in the medicinal plant *Catharanthus roseus*. *The Plant Journal (Pending Publication)*.

Van Moerkercke, A., Steensma, P., Schweizer, F., Pollier, J., Gariboldi, I., Payne, R., … Goossens, A. (2015). The bHLH transcription factor BIS1 controls the iridoid branch of the monoterpenoid indole alkaloid pathway in *Catharanthus roseus*. *Proceedings of the National Academy of Sciences of the United States of America*, *112*(26), 201504951.

Vazquez-Flota, F., De Carolis, E., Alarco, A. M., & De Luca, V. (1997). Molecular cloning and characterization of desacetoxyvindoline-4-hydroxylase, a 2-oxoglutarate dependent-dioxygenase involved in the biosynthesis of vindoline in *Catharanthus roseus* (L.) G. Don. *Plant Molecular Biology*, *34*(6), 935–948.

Verma, A. K., Singh, R. R., & Singh, S. (2012). Cytogenetic effect of EMS on root meristem cells of *Catharanthus roseus* (L.) G. Don var. Nirmal. *International Journal of Pharmacy and Biological Science*, *2*(1), 20–24.

Verpoorte, R., van der Heijden, R., & Moreno, P. R. H. (1997). Chapter 3 Biosynthesis of Terpenoid Indole Alkaloids in *Catharanthus roseus* Cells. *Alkaloids: Chemistry and Pharmacology*, *49*(C), 221–299.

Vogelmann, K., Drechsel, G., Bergler, J., Subert, C., Philippar, K., Soll, J., … Hoth, S. (2012).

Early senescence and cell death in Arabidopsis saul1 mutants involves the PAD4-Dependent salicylic acid pathway. *Plant Physiology*, *159*(August), 1477–1487.

Yang, T. F., Gonzalez-Carranza, Z. H., Maunders, M. J., & Roberts, J. A. (2008). Ethylene and the regulation of senescence processes in transgenic Nicotiana sylvestris plants. *Annals of*

Yu, F., & De Luca, V. (2013). ATP-binding cassette transporter controls leaf surface secretion of anticancer drug components in *Catharanthus roseus*. *Proceedings of the National Academy of Sciences of the United States of America*, *110*(39), 15830–5.

Zhu, J., Wang, M., Wen, W., & Yu, R. (2015). Biosynthesis and regulation of terpenoid indole alkaloids in *Catharanthus roseus*. *Pharmacognosy Reviews*, *9*(17), 24–28.

Zwenger, S., & Basu, C. (2008). Plant terpenoids : applications and future potentials. *Biotechnology and Molecular Biology Reviews*, *3*(February), 1–7.